The aryl hydrocarbon receptor and interferon gamma generate antiviral states via transcriptional repression

Tonya Kueck[1], Elena Cassella[1], Jessica Holler[3], Baek Kim[3,4], Paul D. Bieniasz[1,2]

[1]Laboratory of Retrovirology, The Rockefeller University, New York, New York, United States of America

[2]Howard Hughes Medical Institute, The Rockefeller University, New York, New York, United States of America

[3]Center for Drug Discovery, The Department of Pediatrics, Emory University, Atlanta, Georgia, United States of America

[4]Department of Pharmacy, Kyung Hee University, Seoul, South Korea

Summary

The aryl hydrocarbon receptor (AhR) is a ligand-dependent transcription factor whose activation induces the expression of numerous genes, with many effects on cells. However, AhR activation is not known to affect the replication of viruses. We show that AhR activation in macrophages causes a block to HIV-1 and HSV-1 replication. We find that AhR activation transcriptionally represses cyclin-dependent kinase (CDK)1/2 and their associated cyclins, thereby reducing SAMHD1 phosphorylation, cellular dNTP levels and both HIV-1 and HSV-1 replication. Remarkably, a different antiviral stimulus, interferon gamma (IFN-γ), that induces a largely non-overlapping set of genes, also transcriptionally represses CDK1, CDK2 and their associated cyclins, resulting in similar dNTP depletion and antiviral effects. Concordantly, the SIV Vpx protein provides complete and partial resistance to the antiviral effects of AhR and IFN-γ, respectively. Thus, distinct antiviral signaling pathways converge on CDK/cyclin repression, causing inhibition of viral DNA synthesis and replication.

KEYWORDS

Aryl hydrocarbon receptor, interferon gamma, human immunodeficiency virus, herpes simplex virus, cyclin-dependent kinase, SAMHD1

INTRODUCTION

Hosts have adopted numerous strategies to hinder the replication of invading bacterial or viral pathogens. Indeed, a diverse set of intrinsic or innate immune defense mechanisms enable detection and destruction of foreign protein or nucleic acid associated molecular patterns, and the production of antiviral cytokines. The antiviral cytokines induce expression of genes whose products have antiviral activity, facilitate the recruitment of immune cells and activate the adaptive immune system for the establishment of protective immunological memory [1]. Like many viruses, the human and simian immunodeficiency viruses (HIV and SIV) have acquired various mechanisms to defeat intrinsic, innate and adaptive immunity [2,3].

Key components of the innate defenses against viruses are induced by interferons (IFN), that elicit the expression of antiviral interferon-stimulated genes (ISGs) resulting in the so called 'antiviral state' [4,5]. Most attention has been given to how type-I IFNs inhibit viral infection, and a number of proteins with anti HIV-1 activity are known to be type-I ISGs. Conversely, type-II IFN (IFN-γ) is thought to facilitate protection largely through immunomodulatory rather than directly antiviral mechanisms [6]. Nonetheless, IFN-γ production is induced in the initial stages of HIV-1 infection [7] and some reports indicate that IFN-γ possesses anti-HIV-1 activity, particularly in macrophages [8–11]. Nevertheless, the molecular mechanisms underlying inhibition by IFN-γ have been only partly elucidated [5,12].

In addition to cytokines, other endogenous and exogenous substances, modulate the immune responses to viruses. The aryl hydrocarbon receptor (AhR) is a ligand-dependent transcription factor that is activated by a range of organic molecules of endogenous and exogenous origin, including environmental toxins, tryptophan metabolites, and products of the microbiome [13,14]. In response to ligand activation, AhR translocates from the cytoplasm into the nucleus where it induces the transcription of numerous target genes including detoxifying monooxygenases CYP1A1 and CYP1B1, as well as its own negative regulator, the AhR repressor (AHRR) [13]. AhR activation can have a variety of effects on

cell physiology, impacting proliferation and differentiation [15,16]. In the immune system, AhR activation has modulatory activities including exerting effects on cytokine secretion [13,17]. Additionally, AhR was recently identified as a pattern-recognition receptor for bacterial pigments [18]. AhR signaling can reduce type-I IFN antiviral immune responses [19] and AhR expression is induced in astrocytes by type-I IFN, leading to the suppression of inflammation in the central nervous system [20].

Indoleamine 2,3-dioxygenase 1 (IDO1), is among the most strongly upregulated genes following IFN-γ stimulation. Interestingly, IDO1 catalyzes the initial and rate limiting step in conversion of L-tryptophan into kynurenine [21], is upregulated during HIV-1 infection or IFN-γ stimulation [22] and can block the replication of HIV-1 and other viruses through the inhibition of viral protein production by L-tryptophan depletion [5,23,24]. IDO1 is also thought to be responsible for the generation tryptophan-derived endogenous AhR ligands (Zelante et al., 2014; Romani et al., 2014), raising the possibility of cross-talk between IFN-γ and AhR induced pathways. Nevertheless, while the effects of AhR activation on regulation of immune responses has been frequently studied [13,17], it is not known whether or how AhR activation, and the genes that it induces, affect the replication of viruses.

Here, we investigated whether and how AhR and IFN-γ affect HIV-1 replication in primary cells. We show that AhR and IFN-γ stimulation have little or no effect on HIV-1 replication in T-cells, but both profoundly inhibit HIV-1 replication in macrophages. While AhR agonists and IFN-γ activate the transcription of sets of genes that are nearly completely distinct from each other, we find that both stimuli downregulate the transcription of CDK1, CDK2 and associated cyclins. These transcriptional suppression activities of AhR and IFN-γ reduce the phosphorylation of SAMHD1, activating its dNTP triphosphohydrolase (dNTPase) activity and reduce cellular dNTP levels. Concordantly, the replication of a completely distinct virus that depends on dNTPs for replication, namely herpes simplex virus-1 (HSV-1), is also inhibited by both AhR activation and IFN-γ. SIV Vpx, confers resistance to inhibition by AhR agonists and IFN-γ. Thus, two distinct signaling pathways induce an antiviral state through the activation of SAMHD1 and consequent lowering the levels of cellular dNTP required for viral DNA synthesis.

RESULTS

AhR activation inhibits HIV-1 replication in human macrophages

While immune modulation by AhR ligands has been extensively studied [13,17], the impact of AhR activation on intrinsic host defenses against viral infections is unknown. To determine the impact of AhR activation on HIV-1 replication, we infected primary cells with HIV-$1_{NL\text{-}YU2}$, a cloned HIV-1 bearing the R5-tropic envelope protein from the YU2 isolate or HIV-$1_{89.6}$, a cloned primary dual-tropic HIV-1 isolate, 89.6. Replication of HIV-$1_{NL\text{-}YU2}$ or HIV-$1_{89.6}$ in CD4+ T cells or unfractionated peripheral blood mononuclear cells (PBMC) was unaffected by treatment with the naturally occurring AhR agonist 6-Formylindolo(3,2-b)carbazole (FICZ) or the synthetic AhR antagonist CH-223191 (**Figure 1A and Figure 1-figure supplement 1A-D**). Conversely, replication of both HIV-1 strains in macrophages was inhibited by 10- to 1000-fold, depending on the donor and virus strain used (**Figure 1B and Figure 1-figure supplement 1E-H**). In macrophages from some donors, the AhR antagonist enhanced HIV-1 replication (**Figure 1-figure supplement 1E)**.

To determine at which step the AhR agonist blocked the HIV-1 replication cycle, we executed single cycle infection experiments using a VSV-G pseudotyped HIV-1-GFP reporter virus, that expresses GFP in infected cells. There were ~3 fold fewer GFP+ infected cells when macrophages were pretreated with FICZ (AhR agonist) and ~3-fold more GFP+ infected cells when macrophages were pretreated with CH-223191 (AhR antagonist), compared to the control-treated macrophages (**Figure 1C**). Thus, AhR activation blocked virus replication at early step in the replication cycle, prior to the onset of early gene expression. Next, we used quantitative PCR assays to monitor HIV-1 DNA synthesis during HIV-1 infection of macrophages, and found that it was profoundly inhibited by AhR activation. Indeed, levels of late reverse transcripts in infected FICZ-treated macrophages were similar to those in macrophages treated with the reverse transcription inhibitor nevirapine (**Figure 1D**). Taken together, these data indicated that AhR activation in human macrophages imparts a block to HIV-1 replication that is imposed before or during reverse transcription.

AhR activation can have a variety of effects on cells that could plausibly lead to inhibition of HIV-1 infection, including STAT1 activation (that might active expression of antiviral genes) or inhibition of cell cycle progression [27]. However, we found that AhR activation in macrophages did not induce STAT1 phosphorylation, whereas control IFN-γ-treated macrophages exhibited increased STAT1 phosphorylation (**Figure 1-figure supplement 2A**). Moreover, the differentiated macrophages used in these experiments were found to be exclusively in G0/G1 phases of the cell cycle a state that was unaffected by AhR agonist or antagonist treatment (**Figure 1-figure supplement 2B**). In an attempt to identify candidate effectors of the apparent antiviral action of AhR, we used microarrays to measure changes in mRNA levels induced by treatment of human macrophages with the AhR agonist (**Figure 1E, Figure 1-figure supplement 2C,D and Table S1**). The top fourteen overlapping genes that were represented in AhR agonist-upregulated genes in macrophages from at least 2 donors were selected. These fourteen genes were introduced into the monocyte cell line U937 using a retroviral vector, and the cells treated with PMA to induce differentiation into a macrophage-like state prior to infection with HIV-1. However, spreading HIV-1 replication experiments in these cells did not reveal antiviral activity for any of the genes tested (**Figure 1F**).

AhR activation represses the expression of many genes, including CDK1,2 and associated cyclins

AhR is well known to activate the transcription of target genes. However, in addition to the numerous genes that were upregulated in macrophages by the AhR agonist, we noticed that the expression of a number of genes appeared to be repressed (**Figure 1E, Figure 1-figure supplement 2C, D and Table S2)**. An analysis of the cellular and molecular functions associated with the 100 most downregulated genes revealed that some candidate genes were likely important for the cell cycle progression, putatively acting on cell-cycle checkpoints or the G1/S transition **(Table S3)**. Among these downregulated genes, cyclin-dependent kinase CDK1 (also known as CDC2) and associated cyclins A2 and E2, were present in the lists of 100 most repressed genes from three different macrophage donors (**Figure 1E, Figure 1-figure supplement 2C, D and**

Table S2), and were studied in more detail. RT-PCR assays confirmed the that mRNA levels for these genes were reduced by 2.5-fold (CDK2) to 20-fold (CDK1) in AhR-activated macrophages (**Figure 2A**), while a control mRNA encoding CYP1B1 that is known to be induced by AhR activation (reviewed by Stockinger et al., 2014), was upregulated by ~4-fold. Western blot analysis also showed that reduction of CDK1, CDK2 and cyclin A2 mRNA levels was also reflected as reduced protein levels, while cyclin E2 protein levels were maintained (**Figure 2B**). Conversely, in human PBMCs where the antiviral action of the AhR agonist was not observed **(Figure 1-figure supplement 1B-D)**, CDK1/2 protein levels remained unchanged upon AhR activation, whether or not the cells were activated with PHA or were left unstimulated (**Figure 2-figure supplement 3A**).

Repression of CDK1,2 and associated cyclins reduces SAMHD1 phosphorylation and cellular dNTP levels

One of the substrates of CDK1 and CDK2 that was potentially responsible for macrophage specific antiviral effect of their downregulation was the antiviral enzyme, SAM domain and HD domain-containing protein 1 (SAMHD1). Indeed, SAMHD1 has been shown to inhibit HIV-1 and SIV reverse transcription by reducing the levels of dNTPs in dendritic cells, monocytes and macrophages via its dNTP triphosphohydrolase (dNTPase) activity [28–31]. Crucially, SAMHD1 activity is regulated by CDK1/2, with phosphorylation causing inhibition of SAMHD1 tetramerization which in turn reduces dNTPase activity [32,33].

Western blot analyses revealed that SAMHD1 protein levels in macrophages were unaltered by AhR activation. Notably however, the degree to which SAMHD1 was phosphorylated was clearly decreased when macrophages were treated with the AhR agonist (**Figure 2C**), consistent with the finding that CDK1/2 mRNA and protein levels were decreased (**Figure 2A, B**). Conversely, AhR activation had no effect on SAMHD1 protein levels or the degree to which or was SAMHD1 phosphorylated in PBMCs (**Figure 2-figure supplement 3A**).

CDK1/2 mediated SAMHD1 phosphorylation at position T592 impairs tetramerization and dNTPase activity, causing elevated intracellular dNTP concentrations in cycling cells [34,35]. We employed a previously described primer extension assay [36] to measure dNTP levels in AhR agonist treated macrophages. Consistent with the effects of AhR activation on CDK1/2/cyclin levels, and phosphorylation status of SAMHD1, we found that levels of all four dNTPs in macrophages were decreased, by a mean of 3.2-fold, following AhR activation (**Figure 2D**).

AhR activation inhibits HSV-1 viral replication in macrophages

Large double-stranded DNA (dsDNA) viruses, including herpes simplex viruses (HSV), also infect non-dividing cells such as macrophages and, like HIV-1, require cellular dNTPs for viral DNA synthesis. Indeed, SAMHD1 has been shown to inhibit the replication of dsDNA viruses through cellular dNTP depletion [37,38]. We infected AhR activated or control human monocyte-derived macrophages with an HSV-1 strain (KOS) and monitored progeny viral yield and the expression of HSV-1 glycoprotein D (gD), a structural component of the HSV envelope. Lower levels of gD protein were observed in AhR activated macrophages compared to control cells, with the most pronounced differences occurring at 12 h post infection (**Figure 3A**). Measurement of plaque forming units (PFU) in culture supernatant revealed that progeny viral yield was decreased in AhR activated macrophages by 12-fold at 24 h post infection (**Figure 3B**). Notably, HSV-1 infection did not appear to affect the reduction in phosphorylation of SAMHD1 that results from AhR activation (**Figure 3C**). Thus, these data suggest that AhR activation may confer broad inhibition of viruses whose replication depends on DNA synthesis.

SIV_{mac} Vpx abolishes AhR induced inhibition of HIV-1 and SHIV replication

The viral accessory protein Vpx protein is present in HIV-2 and many SIVs, and is incorporated into virions. Vpx facilitates HIV-2 and SIV infection of macrophages by inducing the proteasomal degradation of SAMHD1 [28,29]. If the block in HIV-1 infection induced by AhR activation in macrophages was primarily caused by SAMHD1 dephosphorylation and consequent dNTP depletion, we reasoned that infection in the presence of Vpx should reduce or abolish the inhibitory effect of AhR activation. To test

this idea, we used Vpx-containing and control SIV_{mac251} virus like particles (SIV3+ and SIV3+ ΔVpx) [39] respectively, and treated macrophage target cells to induce SAMHD1 degradation (**Figure 3-figure supplement 4A**).

In macrophages treated with particles lacking Vpx (SIV3+ ΔVpx), infection using a HIV-1_{NL-YU2}-nluc reporter virus was inhibited by ~9-fold by the AhR agonist (**Figure 3D**). Conversely, infection of cells depleted of SAMHD1 by treatment with Vpx containing particles (SIV3+) was both enhanced compared to untreated macrophages and was nearly completely resistant to inhibition by AhR activation (**Figure 3D**). Next we made use of a hybrid simian-human immunodeficiency virus (SHIV) encoding a macrophage-tropic HIV-1 envelope protein in an otherwise SIV_{mac239} background (SHIV AD8) [40], along with a Vpx deleted counterpart to measure effects of AhR activation and Vpx spreading replication. As was the case for HIV-1, the replication of SHIV AD8 lacking Vpx was inhibited by 10 to 100-fold by AhR activation, depending on the macrophage donor (**Figure 3E and Figure 3-figure supplement 4B, C**). Strikingly however, SHIV AD8 encoding an intact Vpx protein was completely resistant to the effects of AhR activation in multiple donors. Together, these results indicate that the presence of Vpx counteracts the effects of AhR activation and suggest that most, if not all, of the antiviral effect of AhR activation is mediated through SAMHD1.

IFN-γ inhibits HIV-1 replication in human macrophages independently of IDO1 and AhR

IFN-γ has been shown to induce both early and late blocks to HIV-1 infection in CD4 + T cells, macrophages and a number of commonly used cell lines [5,8–12]. The mechanisms underlying this inhibition are not well understood. Nevertheless, IFN-γ has been shown to cause a strain-specific, envelope dependent late block in some cell lines [12] and, an IDO1-induced, tryptophan depletion-dependent block in others [5]. However, the mechanisms underlying the inhibition of HIV-1 replication in primary HIV-1 target cells have not been uncovered. Given that IDO1 is known to be upregulated by IFN-γ and is thought to be a key source of AhR agonists [25,26], we investigated how IFN-γ inhibited HIV-1 replication in parallel to our studies of AhR agonist mediated inhibition.

First, we determined the potency with which IFN-γ inhibited HIV-1 replication in macrophages and PBMC. Levels of HIV-1_{NL-YU2} spread in macrophages at 7 days post infection were reduced by IFN-γ in a dose dependent manner, >400-fold by treatment with 1000 U/ml of IFN-γ (**Figure 4A and Figure 4-figure supplement 5A**). Conversely, spread in PBMCs was inhibited by a comparatively modest 7-fold, dependent on the particular donor (**Figure 4B and Figure 4-figure supplement 5B**). Clearly IFN-γ was a much more potent inhibitor of HIV-1 replication in macrophages than in PBMCs (**Figure 4C**).

To identify candidate effectors responsible for the IFN-γ mediated block in macrophages, we compared mRNA transcriptomes in cells that were untreated or treated with IFN-γ (**Figure 4D, Figure 4-figure supplement 5C,D and Table S4**). The most highly induced gene in all three donors tested was IDO1, which was upregulated between 160 to 250-fold by IFN-γ (**Table S4 and Figure 4-figure supplement 6A**). Crucially however, media supplementation with tryptophan, or the IDO1 inhibitor 1-Methyl-L-tryptophan had no effect on HIV-1 replication (**Figure 4-figure supplement 6B, C**) or AhR activation (**Figure 4-figure supplement 6D, E**), suggesting that the IFN-γ mediated block to HIV-1 in macrophages is different to that resulting from L-tryptophan depletion in T cell lines. Moreover, this finding also suggested that IFN-γ/IDO1 driven generation of kynurenine or other AhR ligands from tryptophan metabolites was not responsible for the inhibition of HIV-1 via AhR activation. Indeed, RT-PCR and microarray analyses revealed that the AhR target gene CYP1B1 was not induced by IFN-γ (**Figure 5A and Figure 5-figure supplement 5C, D**). In fact, the sets of genes induced by AhR activation and IFN-γ treatment were largely non-overlapping (**Table S1 and Table S4**). To determine IFN-γ-induced genes that might be responsible for inhibition, we selected 30 candidate genes that were upregulated in at least three donors (**Table S4**) and expressed them in the monocyte cell line U937. Thereafter, cells were differentiated into a macrophage-like state using PMA, and tested for their ability to support HIV-1 replication. Notably, none of the genes tested had a major effect on HIV-1 replication (**Figure 4E**).

IFN-γ downregulates CDK1, CDK2 and cyclins and thereby activates SAMHD1 in macrophages

Despite the fact that IFN-γ induced a different transcriptional signature than AhR, we noticed that IFN-γ treatment, like AhR activation, caused reduction in the levels of many mRNAs in macrophages (**Figure 4D, Figure 4-figure supplement 5C, D and Table S5**). Given the above findings with AhR, we considered whether the downregulation of particular genes by IFN-γ might play a role in HIV-1 inhibition. Remarkably, and similar to the results obtained with AhR, microarray analyses suggested that CDK1 and cyclin A2 and E2 were among the most strongly downregulated genes following IFN-γ treatment of macrophages (**Table S5**). RT-PCR analyses confirmed that CDK1, CDK2 and associated cyclin A2 and E2 mRNA levels were reduced to varying degrees (2.5-fold to 68-fold) upon IFN-γ treatment (**Figure 5A**). Moreover, western blot analyses indicated that CDK1, CDK2 and cyclin A2 protein levels were reduced in IFN-γ activated macrophages (**Figure 5B**), to a similar degree as in AhR activated cells (**Figure 2B**).

These data suggested that even though IFN-γ treatment does not cause AhR activation, the antiviral pathways triggered by IFN-γ and AhR activation nevertheless converge, in that both treatments lead to transcriptional silencing of CDK1, CDK2 and associated cyclins. Therefore, we investigated whether SAMHD1 might be required for the generation of an IFN-γ induced antiviral state in macrophages. We assessed whether the IFN-γ-mediated reduced levels of CDK1/2 and cyclins observed in IFN-γ treated cells affected the phosphorylation and activity of SAMHD1. Indeed, IFN-γ treatment reduced levels of phosphorylated SAMHD1 while leaving the total levels of SAMHD1 unaffected (**Figure 5D**). There was a commensurate decrease in the level of dNTPs (**Figure 5D**) that was similar in magnitude (2.1-fold to 5.3-fold) to the decrease observed upon AhR activation (**Figure 2D**).

IFN-γ inhibits HIV-1 and HSV-1 replication in macrophages, but SIV Vpx confers resistance to IFN-γ

Consistent with the notion that dNTP depletion is a major contributor to the antiviral activity of IFN-γ in macrophages, we found that HSV-1 replication was inhibited by IFN-γ therein, as was the case with AhR activation. Indeed, IFN-γ treatment resulted in reduced levels of the HSV-1 envelope protein gD in infected cells, as well as reduced yield (30-fold) of infectious progeny virions (**Figure 6A, B**), as was the case with AhR activation (**Figure 3A, B**).

If SAMHD1 dephosphorylation and consequent dNTP depletion contributed to the observed block in HIV-1 infection induced by IFN-γ, then Vpx should confer at least some level of resistance. In single cycle infection experiments, in which macrophages were infected with an HIV-$1_{NL\text{-}YU2}$-nluc reporter virus in the presence of Vpx-null SIV particles, treatment with IFN-γ resulted in a 50-fold inhibition of infection. Conversely, in the presence of Vpx-carrying SIV VLPs, infection HIV-$1_{NL\text{-}YU2}$-nluc was increased compared to Vpx-null SIV particles, and nearly completely resistant to inhibition by IFN-γ (**Figure 6C**). This finding strongly suggested that SAMHD1 is required for the majority of the effect of IFN-γ in single cycle infection assays. In spreading replication experiments with SHIV AD8 or its Vpx-deleted counterpart, conducted in the presence of increasing concentrations of IFN-γ, Vpx again caused substantial, albeit incomplete resistance to the antiviral effects of IFN-γ (**Figure 6D**). These data suggest that the IFN-γ induced antiviral state in macrophages is largely due to reduced SAMHD1 phosphorylation. However, IFN-γ treatment could induce additional blocks to virus replication, resulting in residual sensitivity to IFN-γ in a Vpx-expressing SHIV (**Figure 6C, D**).

CDK1 mRNA turnover is unaffected by AhR and IFN-γ

The antiviral states induced by AhR agonists and IFN-γ were ultimately manifested, in both cases, as a reduction of the steady state levels of CDK1, CDK2, and associated cyclin mRNAs, revealing convergence in the mechanism by which they cause SAMHD1 activation and dNTP depletion. Any reduction in mRNA in steady state level could, in principle, be due to reduced mRNA synthesis (transcription) or increased turnover (degradation). To distinguish between these possibilities, we focused on CDK1, which is

both primarily responsible for SAMHD1 phosphorylation and showed the greatest reduction in mRNA levels in response to AhR activation or IFN-γ signaling. In untreated cells, CDK1 mRNA was depleted with an apparent half-life of several hours following actinomycin D treatment (**Figure 7A**). Conversely, and as expected, control mRNAs encoding TNF-α and IL-1β that are known to be rapidly turned over [41], were quickly depleted following actinomycin D treatment, with a measured half-life of less than one hour in both cases (**Figure 7A**). Notably, there was little or no change in the turnover of CDK1 mRNA following AhR activation or IFN-γ treatment (**Figure 7B**), strongly suggesting that the downregulation of CDK1 mRNA following these stimuli is caused by reduced synthesis rather than increased degradation.

DISCUSSION

Herein we describe an 'antiviral state' in human macrophages that results from AhR agonist or IFN-γ treatment via convergent mechanisms that involve transcriptional repression. While both AhR and IFN-γ are known to increase the expression of a number of target genes, we found that their propensity to repress expression of certain genes was key for their antiviral activity. Specifically, in both cases, transcriptional repression of CDK1, CDK2, and associated cyclins, reduces the degree to which SAMHD1 is phosphorylated and activates its dNTPase activity, thereby reducing the availability of dNTPs that are required for viral DNA synthesis.

AhR is recognized as influencing immune responses to extracellular and intracellular bacteria. Indeed, It has recently been found to be a pattern recognition receptor for pigmented bacterial virulence factors (phenazines and napthoquinones) [18]. AhR deficiency thus increases mouse susceptibility to *Pseudomonas aeruginosa* and *Mycobacterium tuberculosis* infections. Mechanistically, AhR may influence immune responses to bacteria in multiple distinct ways. For example, AhR appears to facilitate the elicitation of anti-bacterial immune responses by regulating the production of IL-22 and other cytokines production by Th17 cells (reviewed by Gutiérrez-Vázquez and Quintana, 2018). AhR also appears to regulate the tissue distribution of lymphocytes [42]. An additional modulatory function of AhR provides protection against immunopathology by

enhancing Treg cell differentiation and cytokine production as well as downregulating inflammation-associated gene expression in dendritic cells to promote 'disease tolerance' [43–45].

Unlike bacteria, viruses are not thought to generate AhR ligands, therefore AhR has not frequently been studied in the context of viral infection. The few prior studies of AhR and viral infection have employed 2,3,7,8-tetrachlorodibenzo-ρ-dioxin (TCDD), an environmental pollutant. While, historically, TCDD was frequently used as a prototypic AhR ligand, it can cause chronic and abnormal AhR activation due to its resistance to degradation by xenobiotic enzymes. In this context, AhR activation during viral infections was reported to exacerbate pathogenesis. For example, TCCD enhanced morbidity and mortality in mice and/or rats infected with influenza A viruses [46], Coxsackievirus [47] or following ocular HSV infection [48]. Exacerbation of viral infection may be related to the fact that AhR activation constrains the type-I interferon response [19]. Other studies have reported that TCDD triggers AhR-dependent HIV-1 gene expression in cell lines, but there has been conflicting data on which HIV-1 promoter elements are responsible (reviewed by Rao and Kumar, 2015).

While viruses are not thought to generate AhR ligands, AhR could nevertheless be activated in macrophages, other myeloid lineage cells or even other cell types, in virus infected individuals through a variety of mechanisms. The array of natural AhR ligands that are known to exist is increasing steadily in number and currently includes ligands provided by diet, commensal microbiota and tryptophan metabolism [13,14]. For example, during HIV-1 infection, CD4+ T cells are rapidly depleted, especially in gut associated lymphoid tissue (GALT). As a likely consequence, the gut microbiome of HIV-1 infected individuals are distinct in composition from healthy individuals [50,51]. Furthermore, dysbiosis and T cell depletion in HIV-1 infected patients may lead to the breakdown of the intestinal barrier, leading to the systemic distribution of bacterial products, as evidenced by increased circulating lipopolysaccharide (LPS) levels [52]. It is plausible, even likely, that increased gut permeability would lead to the increased dissemination of bacteria-derived AhR ligands.

IDO1 may be another source of AhR ligands. IFN-γ treatment of macrophages dramatically upregulates expression of IDO1, and the major pathway of tryptophan metabolism is controlled by IDO1 as well as tryptophan 2,3-dioxygenase (TDO), both of which generate the metabolite kynurenine [13]. Kynurenine is a low affinity AhR agonist and its role as AhR activator under physiological conditions unclear [53]. Indeed, in our experiments, we found no evidence for IFN-γ-induced, IDO1-mediated, AhR activation, suggesting the absence of crosstalk between IFN-γ and AhR antiviral pathways in human macrophages. However, a caveat to this notion is that our experiments were carried out in monolayered cell cultures. It is possible that in the context of a human tissue, with accompanying higher cell densities, that IDO1 metabolites could reach levels required to elicit an AhR response. Indeed, under some circumstances, kynurenine can be produced in large quantities and can drive AhR-mediated suppression of anti-tumor immune responses [53]. The physiological AhR ligand used herein (FICZ) is formed by photolysis of tryptophan and has an affinity for AhR similar to that of TCDD. FICZ is found particularly in the skin, but is also detected in human urine.

Our results demonstrate that AhR activation by this natural AhR ligand results in an inhibition of viral replication in macrophages. The effect of AhR and IFN-γ on HIV-1 replication was clearly cell-type specific, in that the large inhibitory activities seen in macrophages were greatly diminished or absent in CD4+ T cells. The propensity of AhR ligands and IFN-γ to deplete dNTPs should be determined by levels of AhR and IFN-γ receptor, as well as SAMHD1 levels and dNTP concentrations. Notably, AhR, IFN-γ receptor and SAMHD1 are expressed in many tissues and cell types, but SAMHD1 is especially abundant in myeloid and lymphoid cells and is induced by IFN-γ in some cell types [54,55]. Levels of dNTPs are determined both by dNTP degrading SAMHD1 and synthesizing (e.g. ribonucleotide reductase) enzymes, and are unlikely to be sufficiently low in actively dividing cells for the antiviral activities documented herein to be exerted [56]. Rather, non-dividing cells with intrinsically low dNTP levels are likely to provide situations in which dNTP-lowering antiviral strategies are effective. Prior work has demonstrated that dNTPs are 20- to 300-fold lower in macrophages compared to activated PBMC [36,56].

However, the levels of dNTPs in terminally differentiated or non-dividing cells and in other *in vivo* tissues is surprisingly poorly characterized [56]. Thus, further experimentation will be required to determine whether the antiviral activities of AhR and IFN-γ documented herein are widespread among tissues or confined to cells of the myeloid lineage.

Unfortunately, delivery of reporter constructs into macrophages via various methods so altered their responsiveness to AhR ligands and IFN-γ that we were unable to probe effects of AhR activation and IFN-γ treatment on CDK1 promoter activity. Nevertheless, our finding that CDK1 mRNA turnover was unaltered by AhR and IFN-γ, while steady state mRNA levels were reduced by >10-fold indicates that the rate of CDK1 mRNA synthesis must be reduced by AhR ligands and IFN-γ. Further work will be required to determine precisely how transcriptional repression is achieved. Previous work has suggested that $p27^{Kip1}$ can be induced by TCDD-mediated AhR activation, resulting in cell cycle arrest [57], while other studies demonstrated that TCDD treatment of human or mouse cancer cell lines resulted in the recruitment of AhR to E2F-dependent promoters with subsequent repression through a mechanism involving displacement of p300 [58]. It is possible that these affects are related to our findings of CDK/cyclin downregulation, particularly since the CDK1 promoter contains functional E2F binding sites [59–61]. IFN-γ has been shown to induce a cell cycle arrest in various tumor cells by multiple cell type-dependent pathways, including via upregulation of cyclin-dependent kinase inhibitors $p21^{WAF1/Cip1}$ and $p27^{Kip1}$, the signal transducer and activator of transcription-1 (STAT1) signaling pathway or through the activation of E2F transcription factor proteins via $p21^{WAF1/Cip1}$ [62]. Further work will determine how these phenomena are related to the downregulation of CDK/cyclin expression documented herein.

While IFN-γ is largely thought of as an immunoregulatory cytokine, some reports have documented antiviral activity against various viruses, including HIV-1. However, the mechanisms underlying antiviral activity have largely proven elusive [12]. IFN-γ has been shown to play an important role in HSV-1 pathogenesis [63], but the mechanisms by which it inhibits virus replication is seen as largely via largely through modulation of innate and adaptive cellular responses rather than directly affecting viral replication. For HIV-1, IFN-

γ has been shown to be directly antiviral, and cause both early and late blocks to replication. While the early block was poorly characterized, late blocks have been shown to result in part from IDO1 dependent tryptophan starvation [5]. Another IFN-γ imposed late block was shown to be cell-type and viral strain-dependent, with viral determinants mapping to the *env* gene [12]. It is likely that previously described early blocks, that were observed in monocytoid cell lines, are mechanistically the same at that described herein for primary macrophages.

A number of different stimuli or signals, including the DNA damage response [64], AhR ligands and IFN-γ signaling appear to converge on dephosphorylation of SAMHD1. Indeed, immediately before submission of this manuscript another group reported that Type-I, II and III interferon can induce SAMHD1 dephosphorylation [65]. In principle, each of these signaling pathways could be activated as a consequence of infection by retroviruses or DNA viruses. Thus, dephosphorylation of SAMHD1 and consequent dNTP depletion may be a common strategy to limit retrovirus or DNA virus replication. As such targeted activation of AhR, or CDK downregulation via other means may represent a viable antiviral therapeutic strategy.

METHODS

Cells

Fresh human peripheral blood mononuclear cells (PBMCs) were isolated by Ficoll-Paque gradient centrifugation, and plated in serum-free medium for 3 h at 37 °C. The non-adherent cells were discarded and adherent monocytes were cultured in RPMI (Gibco) with 10% FCS (Sigma) and recombinant human granulocyte macrophage colony-stimulating factor (GM-CSF) (100 ng/ml, Gibco). Cell differentiation to macrophages was completed after for 4 to 6 days, and cells were treated as indicated at day 7 prior to infection.

Primary CD4+ T cells were isolated from human blood by Ficoll-Paque gradient centrifugation and negative selection (RosetteSep Human CD4+T Cells Enrichment Cocktail, StemCell Technologies). Primary CD4+ T cells and PBMCs were activated with

Phytohemagglutinin-L (2 μg/ml, Sigma) for 48 h, cultured in the presence of interleukin-2 (50 U/ml, PeproTech), and treated as indicated for 16 h prior to infection.

Viruses

The infectious proviral DNA clone HIV-1_{NL-YU2}, as well as derivatives encoding GFP or nluc encoding (in place of *nef*) were used as previously described by [66]. The HIV-$1_{89.6}$ infectious molecular clone of the primary HIV-1 isolate 89.6 was obtained from the NIH AIDS Reagents Program. The SHIV AD8 provirus was kindly provided by Theodora Hatziioannou. SHIV AD8 ΔVpx was generated by mutating residues T2C, G175T, C178T and deleting nucleotide G183 resulting in a mutated start codon, the introduction of 2 stop codons and a frame shift respectively. Vpx-containing and control SIV_{mac251} constructs, SIV3+ and SIV3+ ΔVpx respectively, were kindly provided by Caroline Goujon. An HSV-1 (strain KOS) virus stock were kindly provided by Margaret MacDonald.

For the generation of HIV-1 virus stocks, 293T cells in a 10-cm plate were transfected with 10 μg of proviral plasmid DNA using polyethyleneimine (PolySciences) and placed in fresh medium after 24 h. At 40 h post-transfection, virus-containing cell supernatant was harvested, treated with 100 U of DNase I (Roche) for 1 h at 37 °C in the presence of 10 mM $MgCl_2$, concentrated using Lenti-X Concentrator (Takara), resuspended in RPMI medium without serum and stored at -80 °C. To determine infectious HIV-1 and SHIV titers, serial dilutions of the virus stocks were used to infect TZM reporter cells as previously described by [67].

SIV3+ and SIV3+ ΔVpx virus like particles (VLPs) were produced as described by [39]. Virus containing supernatants were treated with 100 U of DNase I (Roche) for 1 h at 37 °C in the presence of 10 mM $MgCl_2$, purified by ultracentrifugation through a sucrose cushion (20% w/v; 75 min; 4 °C; 28,000 rpm), resuspended in RPMI medium without serum and stored at -80 °C. The amount of VLPs was normalized using a one-step SYBR Green I based PCR-based reverse transcriptase (RT) assay, as described previously [40].

HIV-1 and SHIV spreading replication assays

For replication assays in macrophages, 1.5 x 10^5 macrophages were plated in each well of a 24-well plate and treated with 0.3% DMSO (Sigma), 0.5 μM 6-Formylindolo(3,2-b)carbazole (FICZ) (Enzo) or 3 μM CH-223191 (Sigma) or the indicated concentrations (in U/ml) of IFN-γ (Gibco) for 16 h. Thereafter cells were infected with 1.5 x 10^5 IU of (measured on TZM-bl cells) of HIV-1_{NL-YU2}, HIV-$1_{89.6}$, or SHIV AD8. At 6 h post infection, cells were washed and supernatants collected over 8 days. The amount of virus released into the supernatant was quantified using a one-step SYBR Green I based PCR RT assay, as described [40].

For replication assays in lymphocytes, 1 x 10^4 PHA-activated PBMCs or CD4+ T cells were plated in one well of a 96-well plate, treated as described above, infected with 1 x 10^3 IU of HIV-1_{NL-YU2}, HIV-$1_{89.6}$, or SHIV AD8. Supernatants were collected and analyzed as described above. U937 CD4/R5 cells expressing candidate genes were infected in the same way except that cells were treated with 50 ng/ml Phorbol 12-myristate 13-acetate (PMA) (Sigma) 2 days prior to infections.

Measurement of HSV-1 replication

For HSV-1 replication experiments, 8 x 10^5 macrophages were treated with 0.3% DMSO, 0.5 μM FICZ, 3 μM CH-223191 or 1000 U/ml IFN-γ for 16 h, followed by infection with HSV-1 at an MOI of 2. At 1 h post infection, cells were washed, supernatants and cells were collected at 12 and 24 h post infection. HSV-1 titers were determined as described [68].

Incoming virus assay

1 x 10^4 macrophages were plated in one well of a 96-well plate, treated with SIV3+ or SIV3+ ΔVpx virus like particles for 10 h, followed by treatment with 0.3% DMSO, 0.5 μM FICZ, 3 μM CH-223191 or 1000 U/ml of IFN-γ; or indicated amount of L-Tryptophan and 1-Methyl-L-tryptophan (Sigma) for 16 h before infection with NLYU2 nluc. Cells were lysed 48 h post infection and luciferase was measured using the Nano-Glo Luciferase Assay System (Promega) and Modulus II Microplate Multimode Reader (Turner BioSystems).

Measurement of HIV-1 DNA species in infected cells

For analysis of HIV-1 late reverse transcription products in infected cells, 8 x 10^5 macrophages were seeded in 6-well culture plates and infected with 8 x 10^6 IU (as determined on TZM-bl cells) of HIV-1_{NL-YU2}. Cells were either treated with 0.3% DMSO or 0.5 μM FICZ for 16 h prior to infection, or were treated with Nevirapine (Sigma) starting at the time of infection. Total DNA was extracted 24 h post infection, using the NucleoSpin Tissue Kit (Macherey-Nagel). The resulting DNA samples were used as template for quantitative PCR using TaqMan Gene Expression Master Mix (Applied Biosystems) and StepOne Plus Real-Time PCR system (Applied Biosystems). The primer pairs and PCR conditions used in this study were as described previously [69].

Microarray Analysis

Total RNA was extracted, using the RNeasy Plus Mini Kit (QIAGEN), from human macrophages that were treated with 0.3% DMSO (Sigma), 0.5 μM 6-Formylindolo(3,2-b)carbazole (alternative name FICZ) (Enzo) or 3 μM CH-223191 (Sigma) for 24 h before harvest. Alternatively, macrophages were either untreated or treated with 1000 U/ml IFN-γ (Gibco) for 24 h before harvest. Complementary RNA was prepared and probed using HumanHT-12 v4.0 Gene Expression BeadChips (Illumina), according to manufacturer's instructions.

Stable expression of individual genes

A U937-derived cell line expressing human CD4 and CCR5 as a single transcript linked by a self-cleaving picornovirus-derived 2A peptide-encoding sequence was generated by transduction with pLHCX followed by selection with 50 μg/ml Hygromycin B. A single cell clone was derived from the population of transduced cells by limiting dilution. For constitutive expression of genes induced in the AhR and IFN-γ microarrays, a lentiviral vector, CSIB, was derived from CSGW by replacing sequences encoding GFP with a multi-cloning site followed by an IRES sequence and a blasticidin resistance cassette. A selection of genes that were induced by 0.5 μM FICZ or 1000 U/ml IFN-γ were cloned into CSIB and were introduced into the U937 cells with CSIB based viruses followed by

selection with 5 µg/ml blasticidin. A control cell line containing empty vector CSIB was similarly generated. The genes analyzed by this method were GPR183, CXCR5, ADK, COL23A1, CYGB, RASAL1, NCF1, SEMA6B, TNFAIP8L3, SLC7A11, XYLT, FUCA1, LRG1, ITGB7, ANKRD22, CCL7, CD40, FCGR1A, GIMAP8, FCGR1B, FGL2, RABGAP1L, PST-PIP2, PSME2, GIMAP6, HAPLN3, IL27, LYSMD2, MAP3K7CL, NFIX, NUPR1, GPBAR1, TMEM110, UBD, C5, SCIMP, SDS, SOD2, STAMBPL1, CIITA, JUP, PARP14 and METTL7B.

Measurement of mRNA levels using PCR

Macrophages (8 x 10^5) were treated with 0.3% DMSO, 0.5 µM FICZ, 3 µM CH-223191 or 1000 U/ml IFN-γ for 24 h, and RNA was isolated using the NucleoSpin RNA Kit (Macherey-Nagel). cDNA was synthesized with SuperScript III First-Strand Synthesis System (Invitrogen), and analyzed by quantitative PCR using TaqMan Gene Expression Master Mix (Applied Biosystems). Duplicate reactions were run according to manufacturer's instructions using a StepOne Plus Real-Time PCR system (Applied Biosystems). For relative quantification, samples were normalized to GAPDH. The following TaqMan Gene Expression Assays (Applied Biosystems) were used: GAPDH (Hs02786624_g1), CYP1B1 (Hs00164383_m1), CDK1 (Hs00938777_m1), CDK2 (Hs01548894_m1), CCNA2 (Hs00996788_m1), CCNE2 (Hs00180319_m1).

Western blotting

Cells were lysed in LDS sample buffer (Invitrogen), separated by electrophoresis on NuPage 4-12% Bis-Tris gels (Invitrogen) and blotted onto nitrocellulose membranes (GE Healthcare). Membranes were incubated with rabbit anti-HSP90 (Santa Cruz Biotechnology), mouse anti-SAMHD1 (OriGene), rabbit anti-pSAMHD1 (ProSci), mouse anti-cdc2 (Cell Signaling), rabbit anti-CDK2 (proteintech), rabbit anti-CCNE2 (proteintech), rabbit anti-cyclin A2 (proteintech), rabbit anti-STAT1 (proteintech), rabbit anti-pSTAT1 (Cell Signaling), mouse anti-HSV-1 gD (Santa Cruz Biotechnology) or mouse anti-IDO1 (proteintech). Thereafter, membranes were incubated with goat anti-rabbit IRDye 800CW and goat anti-mouse IRDye 680RD (respectively LI-COR Biosciences), and scanned using a LI-COR Odyssey infrared imaging system.

Alternatively, membranes were incubated with appropriate horseradish peroxidase (HRP) conjugated secondary antibodies (Jackson ImmunoResearch), and visualized using SuperSignal West Femto Chemiluminescent solution (Thermo Fisher) and a C-DiGit Western Blot Scanner.

Whole-cell dNTP quantification

Macrophages were plated at 5 x 10^6 cells per 10-cm dish, treated with 0.3% DMSO, 0.5 μM FICZ, 3 μM CH-223191 or 1000 U/ml IFN-γ for 24 h, washed in 1x PBS and lysed in 65% methanol. Whole-cell dNTP contents were measured using a single nucleotide incorporation assay, as described [36].

Measurement of mRNA stability

Macrophages (6 x 10^5) were treated with 5 μg/ml actinomycin D (Sigma) in combination with 0.3% DMSO, 0.5 μM FICZ, 3 μM CH-223191 or 1000 U/ml IFN-γ for indicated amounts of time and mRNA levels were measured as described above. As controls, the following additional TaqMan Gene Expression Assays (Applied Biosystems) were used: TNF (Hs00174128_m1) and IL1B (Hs01555410_m1).

ACKNOWLEDGMENTS

We thank Theodora Hatziioannou for the SHIV AD8 proviral plasmid, Caroline Goujon for SIV3+ constructs, and NIH AIDS reagents program for HIV-1 infectious molecular clones, João Lucas Duarte and Gitta Stockinger for helpful discussions and Margaret MacDonald for the HSV-1 KOS virus stock. This work was supported by grants from the NIH R37AI64003 (to P.D.B.), R01 GM104198 (to B.K.) and R01 AI136581 (to B.K.). The content of this manuscript is solely the responsibility of the authors and does not necessarily represent the official views of the National Institutes of Health.

AUTHOR CONTRIBUTIONS

T.K. and P.D.B. conceived the study, designed experiments, analyzed the data, and wrote the paper. T.K., E.C. and J.H. executed the experiments. B.K. and P.D.B. supervised the work.

REFERENCES

1. Stetson DB, Medzhitov R. Type I Interferons in Host Defense. *Immunity*. 2006;25(3). doi:10.1016/j.immuni.2006.08.007.
2. Blanco-Melo D, Venkatesh S, Bieniasz PD. Intrinsic Cellular Defenses against Human Immunodeficiency Viruses. *Immunity*. 2012;37(3):399-411. doi:10.1016/j.immuni.2012.08.013.
3. Malim MH, Bieniasz PD. HIV Restriction Factors and Mechanisms of Evasion. *Cold Spring Harbor perspectives in medicine*. 2012;2(5):a006940. doi:10.1101/cshperspect.a006940.
4. Schoggins JW, Wilson SJ, Panis M, et al. A diverse range of gene products are effectors of the type I interferon antiviral response. *Nature*. 2011;472(7344):481-485. doi:10.1038/nature09907.
5. Kane M, Zang TM, Rihn SJ, et al. Identification of Interferon-Stimulated Genes with Antiretroviral Activity. *Cell Host & Microbe*. 2016;20(3):392-405. doi:10.1016/j.chom.2016.08.005.
6. Roff SR, Noon-Song EN, Yamamoto JK. The significance of interferon-γ in HIV-1 pathogenesis, therapy, and prophylaxis. *Frontiers in Immunology*. 2014;4(JAN). doi:10.3389/fimmu.2013.00498.
7. Stacey AR, Norris PJ, Qin L, et al. Induction of a Striking Systemic Cytokine Cascade prior to Peak Viremia in Acute Human Immunodeficiency Virus Type 1 Infection, in Contrast to More Modest and Delayed Responses in Acute Hepatitis B and C Virus Infections. *Journal of Virology*. 2009;83(8):3719-3733. doi:10.1128/JVI.01844-08.
8. Hammer SM, Gillis JM, Groopman JE, Rose RM. In vitro modification of human immunodeficiency virus infection by granulocyte-macrophage colony-stimulating factor and gamma interferon. *Proc Natl Acad Sci U S A*. 1986;83(22):8734-8738. doi:10.1073/pnas.83.22.8734.
9. Koyanagi Y, O'Brien W a, Zhao JQ, Golde DW, Gasson JC, Chen IS. Cytokines alter production of HIV-1 from primary mononuclear phagocytes. *Science*. 1988;241(4873):1673-1675. doi:10.1126/science.3047875.
10. Kornbluth RS, Oh PS, Munis JR, Cleveland PH, Richman DD. Interferons and Bacterial Lipopolysaccharide Protect Macrophages From Productive Infection By Human Immunodeficiency Virus in Vitro. *The Journal of experimental medicine*. 1989;169(March):1137-1151.
11. Meylan PRA, Guatelli JC, Munis JR, Richman DD, Kornbluth RS. Mechanisms for the Inhibition of HIV Replication by Interferons-α, -β, and -γ in Primary Human Macrophages. *Virology*. 1993;193:138-148. doi:10.1006/viro.1993.1110.
12. Rihn SJ, Foster TL, Busnadiego I, et al. The Envelope Gene of Transmitted HIV-1 Resists a Late IFNγ-Induced Block. *Journal of Virology*. 2017;91(7):e02254-16. doi:10.1128/JVI.02254-16.

13. Stockinger B, Di Meglio P, Gialitakis M, Duarte JH. The aryl hydrocarbon receptor: multitasking in the immune system. *Annual review of immunology*. 2014;32:403-432. doi:10.1146/annurev-immunol-032713-120245.
14. Zhang L, Nichols RG, Patterson AD. The aryl hydrocarbon receptor as a moderator of host-microbiota communication. *Curr Opin Toxicol*. 2017;2(30–35). doi:10.1016/j.cotox.2017.02.001.
15. Quintana FJ, Basso AS, Iglesias AH, et al. Control of T reg and T H 17 cell differentiation by the aryl hydrocarbon receptor. *Nature*. 2008;453(May):65-72. doi:10.1038/nature06880.
16. Veldhoen M, Hirota K, Westendorf AM, et al. The aryl hydrocarbon receptor links TH17-cell-mediated autoimmunity to environmental toxins. *Nature*. 2008;453(May):106-110. doi:10.1038/nature06881.
17. Gutiérrez-Vázquez C, Quintana FJ. Regulation of the Immune Response by the Aryl Hydrocarbon Receptor. *Immunity*. 2018;48(1):19-33. doi:10.1016/j.immuni.2017.12.012.
18. Moura-Alves P, Faé K, Houthuys E, et al. AhR sensing of bacterial pigments regulates antibacterial defence. *Nature*. 2014;512:387-392. doi:10.1038/nature13684.
19. Yamada T, Horimoto H, Kameyama T, et al. Constitutive aryl hydrocarbon receptor signaling constrains type I interferon–mediated antiviral innate defense. *Nature Immunology*. 2016;17(April):1-10. doi:10.1038/ni.3422.
20. Rothhammer V, Mascanfroni ID, Bunse L, et al. Type I interferons and microbial metabolites of tryptophan modulate astrocyte activity and central nervous system inflammation via the aryl hydrocarbon receptor. *Nature Medicine*. 2016;22(6):586-597. doi:10.1038/nm.4106.
21. Hayaishi O. Properties and function of indoleamine 2,3-dioxygenase. *J Biochem*. 1976;79(4):13-21.
22. Favre D, Mold J, Hunt PW, et al. Tryptophan Catabolism by Indoleamine 2 , 3-Dioxygenase 1 Alters the Balance of T H 17 to Regulatory T Cells in HIV Disease. *Sci Transl Med*. 2010;2(32):32ra36. doi:10.1126/scitranslmed.3000632.
23. Mao R, Zhang J, Jiang D, et al. Indoleamine 2,3-dioxygenase mediates the antiviral effect of gamma interferon against hepatitis B virus in human hepatocyte-derived cells. *J Virol*. 2011;85(2):1048-1057. doi:10.1128/JVI.01998-10.
24. Obojes K, Andres O, Kim KS, Däubener W, Schneider-Schaulies J. Indoleamine 2,3-Dioxygenase Mediates Cell Type-Specific Anti-Measles Virus Activity of Gamma Interferon. *Journal of Virology*. 2005;79(12):7768-7776. doi:10.1128/JVI.79.12.7768-7776.2005.
25. Zelante T, Iannitti RG, Fallarino F, et al. Tryptophan feeding of the IDO1-AhR axis in host-microbial symbiosis. *Frontiers in Immunology*. 2014;5(December):1-4. doi:10.3389/fimmu.2014.00640.
26. Romani L, Zelante T, De Luca A, et al. Microbiota control of a tryptophan-AhR pathway in disease tolerance to fungi. *European Journal of Immunology*. 2014;44(11):3192-3200. doi:10.1002/eji.201344406.
27. Kimura A, Naka T, Nohara K, Fujii-kuriyama Y, Kishimoto T. Aryl hydrocarbon receptor regulates Stat1 activation and participates in the development of Th17 cells. *PNAS*. 2008;105(28):9721-9726.

28. Hrecka K, Hao C, Gierszewska M, et al. Vpx relieves inhibition of HIV-1 infection of macrophages mediated by the SAMHD1 protein. *Nature*. 2011;474(7353):658-661. doi:10.1038/nature10195.
29. Laguette N, Sobhian B, Casartelli N, et al. SAMHD1 is the dendritic- and myeloid-cell-specific HIV-1 restriction factor counteracted by Vpx. *Nature*. 2011;474(7353):654-657. doi:10.1038/nature10117.
30. Yan J, Kaur S, Delucia M, et al. Tetramerization of SAMHD1 Is Required for Biological Activity and Inhibition of HIV Infection. *The Journal of biological chemistry*. 2013;288(15):10406-10417. doi:10.1074/jbc.M112.443796.
31. Delucia M, Mehrens J, Wu Y, Ahn J. HIV-2 and SIVmac Accessory Virulence Factor Vpx Down-regulates SAMHD1 Enzyme Catalysis Prior to. *The Journal of biological chemistry*. 2013;288(26):19116-19126. doi:10.1074/jbc.M113.469007.
32. Hansen EC, Seamon KJ, Cravens SL, Stivers JT. GTP activator and dNTP substrates of HIV-1 restriction factor SAMHD1 generate a long-lived activated state. *PNAS*. 2014:E1843–E1851. doi:10.1073/pnas.1401706111.
33. Ji X, Wu Y, Yan J, et al. Mechanism of allosteric activation of SAMHD1 by dGTP. *Nature structural & molecular biology*. 2013;20(11):1304-1309. doi:10.1038/nsmb.2692.
34. Cribier A, Descours B, Valadão ALC, Laguette N, Benkirane M. Phosphorylation of SAMHD1 by cyclin A2/CDK1 regulates its restriction activity toward HIV-1. *Cell reports*. 2013;3(4):1036-1043. doi:10.1016/j.celrep.2013.03.017.
35. White TE, Brandariz-Nuñez A, Valle-Casuso JC, et al. The retroviral restriction ability of SAMHD1, but not its deoxynucleotide triphosphohydrolase activity, is regulated by phosphorylation. *Cell host & microbe*. 2013;13(4):441-451. doi:10.1016/j.chom.2013.03.005.
36. Diamond TL, Roshal M, Jamburuthugoda VK, et al. Macrophage Tropism of HIV-1 Depends on Efficient Cellular dNTP Utilization by Reverse Transcriptase. *Journal of Biological Chemistry*. 2004;279(49):51545-51553. doi:10.1074/jbc.M408573200.
37. Hollenbaugh JA, Gee P, Baker J, et al. Host Factor SAMHD1 Restricts DNA Viruses in Non- Dividing Myeloid Cells. *PLoS pathogens*. 2013;9(6):e1003481. doi:10.1371/journal.ppat.1003481.
38. Kim ET, White TE, Brandariz-Núñez A, Diaz-Griffero F, Weitzman MD. SAMHD1 Restricts Herpes Simplex Virus 1 in Macrophages by Limiting DNA Replication. *Journal of Virology*. 2013;87(23):12949-12956. doi:10.1128/JVI.02291-13.
39. Goujon C, Schaller T, Galão RP, et al. Evidence for IFN α -induced , SAMHD1-independent inhibitors of early HIV-1 infection. *Retrovirology*. 2013;10(23):1-6.
40. Del Prete GQ, Keele BF, Fode J, et al. A single gp120 residue can affect HIV-1 tropism in macaques. *PLoS pathogens*. 2017;13(9):e1006572. doi:10.1371/journal.ppat.1006572.
41. Mahmoud L, Al-Enezi F, Al-Saif M, Warsy A, Khabar KSA, Hitti EG. Sustained stabilization of Interleukin-8 mRNA in human macrophages. *RNA Biology*. 2014;11(2):124-133. doi:10.4161/rna.27863.
42. Li Y, Innocentin S, Withers DR, et al. Exogenous stimuli maintain intraepithelial lymphocytes via aryl hydrocarbon receptor activation. *Cell*. 2011;147(3):629-640. doi:10.1016/j.cell.2011.09.025.

43. Gandhi R, Kumar D, Burns EJ, et al. Activation of the aryl hydrocarbon receptor induces human type 1 regulatory T cell–like and Foxp3+ regulatory T cells. *Nature Immunology*. 2010;11(9):846-853. doi:10.1038/ni.1915.
44. Apetoh L, Quintana FJ, Pot C, et al. The aryl hydrocarbon receptor interacts with c-Maf to promote the differentiation of type 1 regulatory T cells induced by IL-27. *Nature Immunology*. 2010;11(9):854-861. doi:10.1038/ni.1912.
45. Bessede A, Gargaro M, Pallotta MT, et al. Aryl hydrocarbon receptor control of a disease tolerance defence pathway. *Nature*. 2014;511(7508):184-190. doi:10.1038/nature13323.
46. Lawrence BP, Vorderstrasse BA. New insights into the aryl hydrocarbon receptor as a modulator of host responses to infection. *Seminars in Immunopathology*. 2013;35:615-626. doi:10.1007/s00281-013-0395-3.
47. Funseth E, Wesslén L, Lindh U, Friman G, Ilbäck N-G. Effect of 2,3,7,8-tetrachlorodibenzo-p-dioxin on trace elements, inflammation and viral clearance in the myocardium during Coxsackievirus B3 infection in mice. *Science of The Total Environment*. 2002;284(1-3):135-147. doi:10.1016/S0048-9697(01)00874-9.
48. Veiga-Parga T, Suryawanshi A, Rouse BT. Controlling viral immuno-inflammatory lesions by modulating aryl hydrocarbon receptor signaling. *PLoS Pathogens*. 2011;7(12):e1002427. doi:10.1371/journal.ppat.1002427.
49. Rao PSS, Kumar S. Polycyclic aromatic hydrocarbons and cytochrome P450 in HIV pathogenesis. *Frontiers in Microbiology*. 2015;6(June):1-7. doi:10.3389/fmicb.2015.00550.
50. Bandera A, Benedetto I De, Bozzi G, Gori A. Altered gut microbiome composition in HIV infection : causes , effects and potential intervention. *Current opinion in HIV and AIDS*. 2018;13:73-80. doi:10.1097/COH.0000000000000429.
51. Zilberman-Schapira G, Zmora N, Itav S, Bashiardes S, Elinav H, Elinav E. The gut microbiome in human immunodeficiency virus infection. *BMC Medicine*. 2016;14(83):1-11. doi:10.1186/s12916-016-0625-3.
52. Brenchley JM, Price DA, Schacker TW, et al. Microbial translocation is a cause of systemic immune activation in chronic HIV infection. *Nature Medicine*. 2006;12:1365.
53. Opitz CA, Litzenburger UM, Sahm F, et al. An endogenous tumour-promoting ligand of the human aryl hydrocarbon receptor. *Nature*. 2011;478(7368):197-203. doi:10.1038/nature10491.
54. Li N, Zhang W, Cao X. Identification of human homologue of mouse IFN-gamma induced protein from human dendritic cells. *Immunology Letters*. 2000;74:221-224.
55. Liao W, Bao Z, Cheng C, Mok Y, Wong WSF. Dendritic cell-derived interferon-gamma -induced protein mediates tumor necrosis factor-aplha stimulation of human lung fibroblasts. *Proteomics*. 2008;8:2640-2650. doi:10.1002/pmic.200700954.
56. Amie SM, Noble E, Kim B. Intracellular nucleotide levels and the control of retroviral infections. *Virology*. 2013;436(2):247-254. doi:10.1016/j.virol.2012.11.010.
57. Kolluri S, Weiss C, Koff A. p27 (Kip1) induction and inhibition of proliferation by the intracellular Ah receptor in developing thymus and hepatoma cells. *Genes*

Dev. 1999;13:1742-1753. http://scholar.google.com/scholar?hl=en&btnG=Search&q=intitle:p27+Kip1+induction+and+inhibition+of+proliferation+by+the+intracellular+Ah+receptor+in+developing+thymus+and+hepatoma+cells#0.

58. Marlowe JL, Knudsen ES, Schwemberger S, Puga A. The aryl hydrocarbon receptor displaces p300 from E2F-dependent promoters and represses S phase-specific gene expression. *Journal of Biological Chemistry*. 2004;279(28):29013-29022. doi:10.1074/jbc.M404315200.
59. Dalton S. Cell cycle regulation of the human cdc2 gene. *The EMBO journal*. 1992;11(5):1797-1804. doi:10.1002/J.1460-2075.1992.TB05231.X.
60. Sugarman JL, Schonthal AH, Glass CK. Identification of a cell-type-specific and E2F-independent mechanism for repression of cdc2 transcription. *Mol Cell Biol*. 1995;15(6):3282-3290.
61. Tommasi S, Pfeifer GP. In vivo structure of the human cdc2 promoter: release of a p130-E2F-4 complex from sequences immediately upstream of the transcription initiation site coincides with induction of cdc2 expression. *Molecular and cellular biology*. 1995;15(12):6901-6913.
62. Schroder K, Hertzog PJ, Ravasi T, Hume DA. Interferon-gamma: an overview of signals , mechanisms and functions. *Journal of leukocyte biology*. 2004;75(February):163-189. doi:10.1189/jlb.0603252.Journal.
63. Bigley NJ. Complexity of interferon-gamma interactions with HSV-1. *Frontiers in Immunology*. 2014;5(FEB):1-9. doi:10.3389/fimmu.2014.00015.
64. Mlcochova P, Caswell SJ, Taylor IA, Towers GJ, Gupta RK. DNA damage induced by topoisomerase inhibitors activates SAMHD1 and blocks HIV-1 infection of macrophages. *EMBO Journal*. 2017:1-13. doi:10.15252/embj.201796880.
65. Matthew A. Szaniawski, Spivak AM, Cox JE, et al. SAMHD1 Phosphorylation Coordinates the Anti-HIV-1 Response by Diverse Interferons and Tyrosine Kinase Inhibition. *mBio*. 2018;9(3):e00819-18.
66. Zhang Y, Hatziioannou T, Zang T, et al. Envelope-Dependent , Cyclophilin-Independent Effects of Glycosaminoglycans on Human Immunodeficiency Virus Type 1 Attachment and Infection. *Journal of virology*. 2002;76(12):6332-6343. doi:10.1128/JVI.76.12.6332.
67. Bitzegeio J, Sampias M, Bieniasz PD, Hatziioannou T. Adaptation to the interferon-induced antiviral state by human and simian immunodeficiency viruses. *Journal of virology*. 2013;87(6):3549-3560. doi:10.1128/JVI.03219-12.
68. Bick MJ, Carroll JN, Gao G, et al. Expression of the Zinc-Finger Antiviral Protein Inhibits Alphavirus Replication. *Journal of Virology*. 2003;77(21):11555-11562. doi:10.1128/JVI.77.21.11555.
69. Butler SL, Hansen MS, Bushman FD. A quantitative assay for HIV DNA integration in vivo. *Nature medicine*. 2001;7(5):631-634. doi:10.1038/87979.

FIGURES

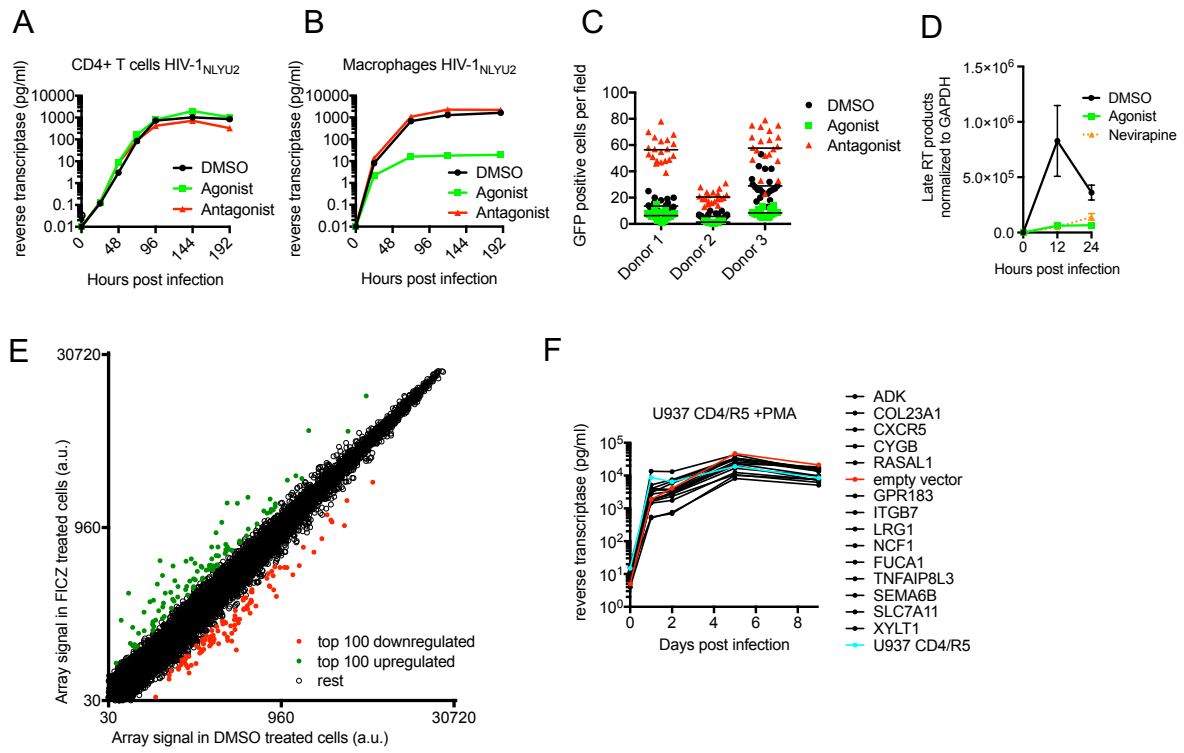

Figure 1: AhR activation inhibits HIV-1 replication in macrophages

(A and B) HIV-1_{NLYU2} replication in CD4+ T cells (A) or macrophages (B) treated with AhR agonist or antagonist. Representative of at least 3 different donors.

(C) Numbers of infected macrophages after HIV-1_{NLYU2}-GFP single-round infection. Each symbol represents a single field in which numbers of infected cells were counted.

(D) Quantitative PCR analysis of late HIV-1 DNA (late reverse transcripts (RT)) abundance in macrophages. Error bars represent standard deviation, n=4.

(E) Microarray analysis of RNA extracted from macrophages treated with AhR agonist or control. The array signal is plotted in arbitrary units (a.u.).

(F) HIV-1_{NLYU2} replication in a PMA-differentiated monocytic cell line (U937 CD4/ R5) transduced with a lentiviral vectors (CSIB) expressing the indicated genes that were upregulated in response to the AhR agonist (from (E)). Representative example of 2 independent experiments.

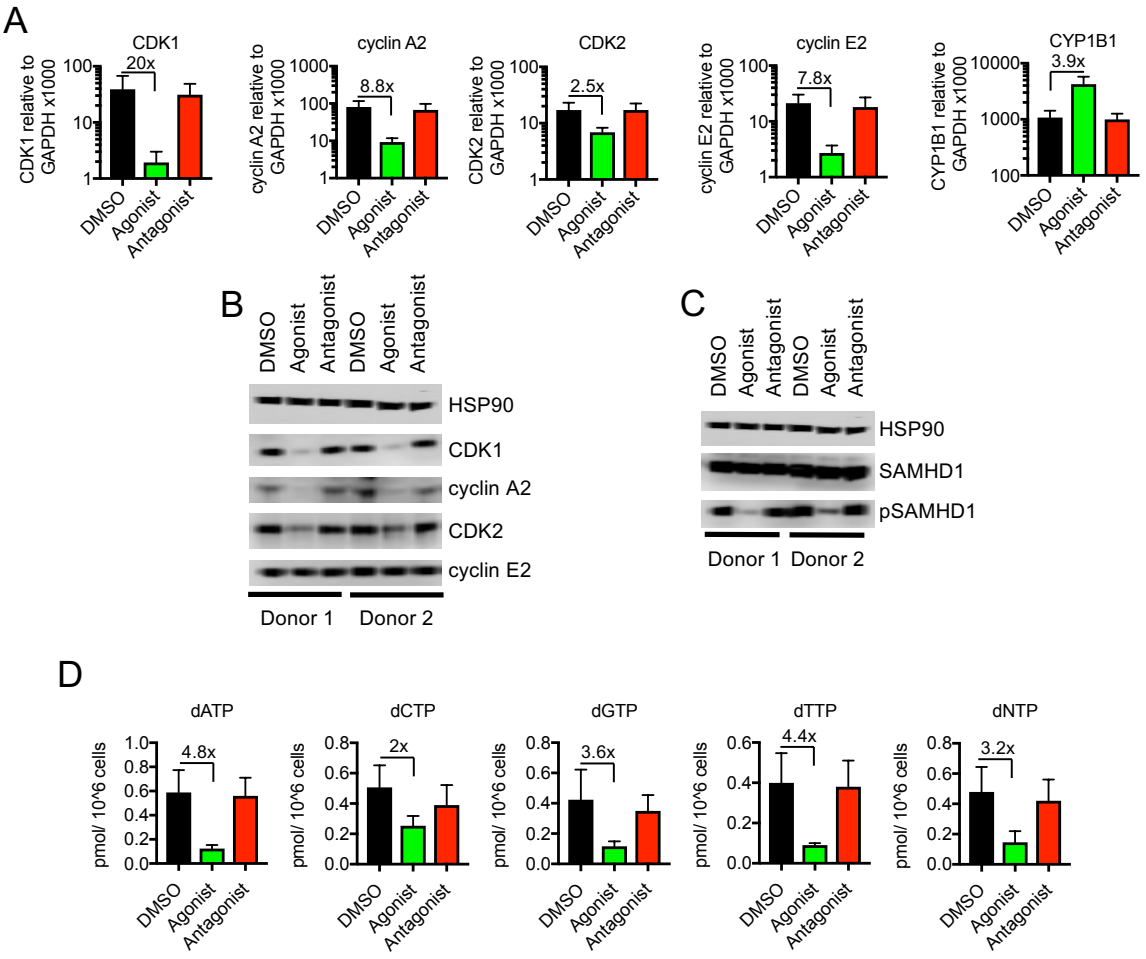

Figure 2: Reduced CDK/cyclin, phospho-SAMHD1 and dTNP levels in macrophages following activation of AhR

(A) Quantitative PCR analysis of CDK1, cyclin A2, CDK2, cyclin E2 and CYP1B1 mRNA levels in macrophages treated with carrier (DMSO), AhR agonist or antagonist. Values indicate fold-change, error bars represent standard deviation of data from 5 different donors.

(B) Western blot analysis of HSP90 (loading control) CDK1, cyclin A2, CDK2, cyclin E2 protein levels in macrophages treated with carrier (DMSO), AhR agonist or antagonist.

(C) Western blot analysis of HSP90 (loading control), total SAMHD1 levels, and phosphorylated SAMHD1 levels in macrophages treated with carrier (DMSO), AhR agonist or antagonist.

(D) Analysis of dNTP levels in macrophages treated with AhR agonist or antagonist. Error bars represent standard deviation of data from 3 different donors, numbers indicate fold change.

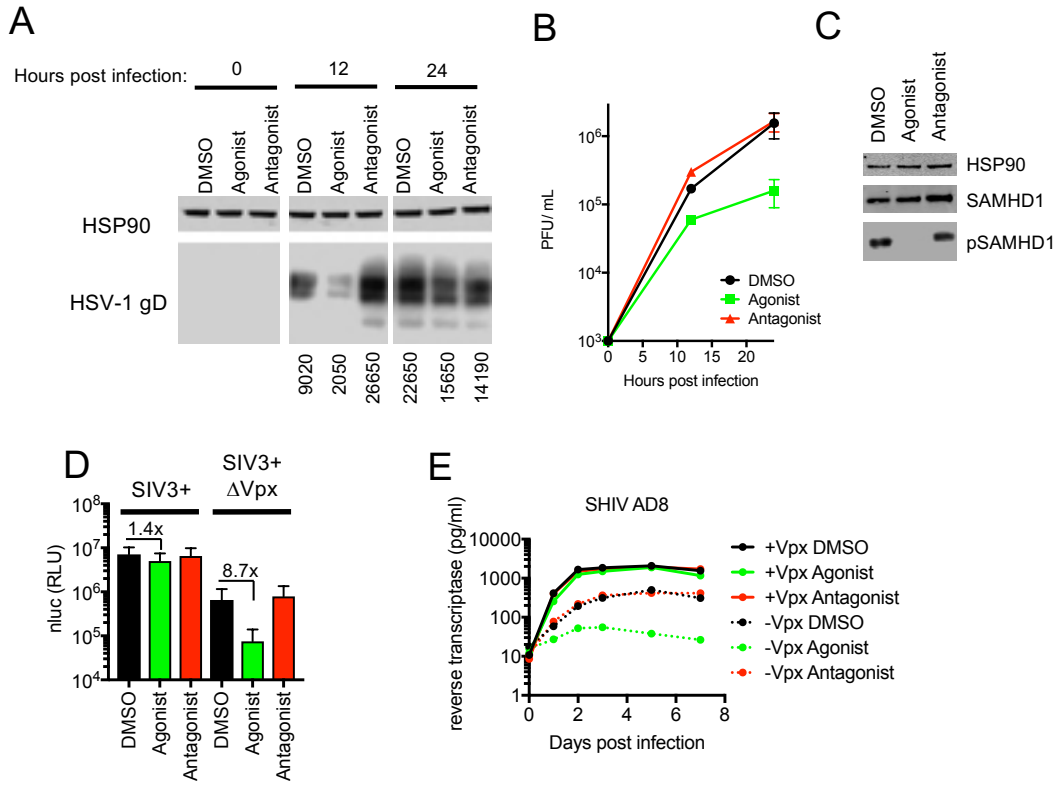

Figure 3: AhR activation inhibits HIV-1 and HSV-1 replication, but SIV_{mac} Vpx confers resistance

(A) Western blot analysis of HSV-1 glycoprotein D (gD) levels over time in infected macrophages treated with AhR agonist or antagonist. Numbers represent relative band intensities. Representative of 2 different donors.

(B) HSV-1 infectious virion yield during replication in macrophages treated as in (A). Error bars represent standard deviation, n=2.

(C) Western blot analysis of SAMHD1 and phospho-SAMHD1 levels in HSV-1 infected macrophages treated with AhR agonist or antagonist. Representative of 2 different donors.

(D) Single round virus replication in macrophages treated with SIV3+ or SIV3+ ΔVpx virus like particles and AhR agonist or antagonist before infection with $HIV\text{-}1_{NLYU2}$-nluc. Error bars represent standard deviation of data from 6 different donors, numbers indicate fold change.

(E) Supernatant reverse transcriptase levels in macrophages treated with AhR agonist or antagonist and infected with chimeric SHIV AD8 expressing or not expressing the Vpx protein. Representative of 3 different donors.

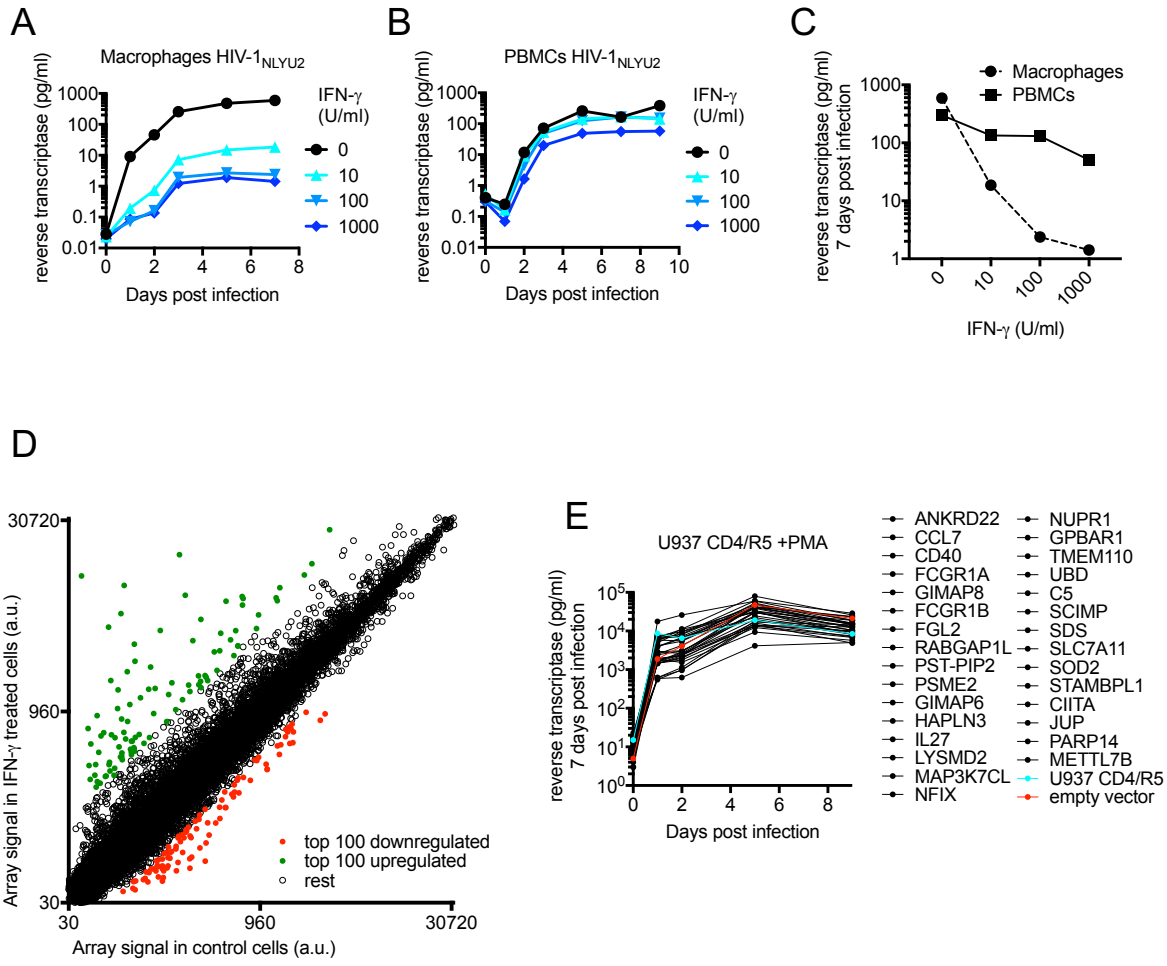

Figure 4: IFN-γ inhibits HIV-1 replication in macrophages

(A and B) HIV-1_{NL-YU2} replication in macrophages (A) or PBMCs (B) treated with increasing concentrations of IFN-γ. Representative of 3 different donors.

(C) Comparison of HIV-1 supernatant reverse transcriptase levels, at seven days after infection in infected macrophages or PBMCs treated with increasing concentrations of IFN-γ from (A and B).

(D) Microarray analysis of RNA extracted from macrophages treated with IFN-γ or control. The array signal is plotted in arbitrary units (a.u.).

(E) HIV-1_{NL-YU2} replication in a PMA treated monocytic cell line (U937 CD4/ R5) transduced with lentiviral vectors (CSIB) expressing the indicated upregulated genes from (D). Representative example of 2 independent experiments.

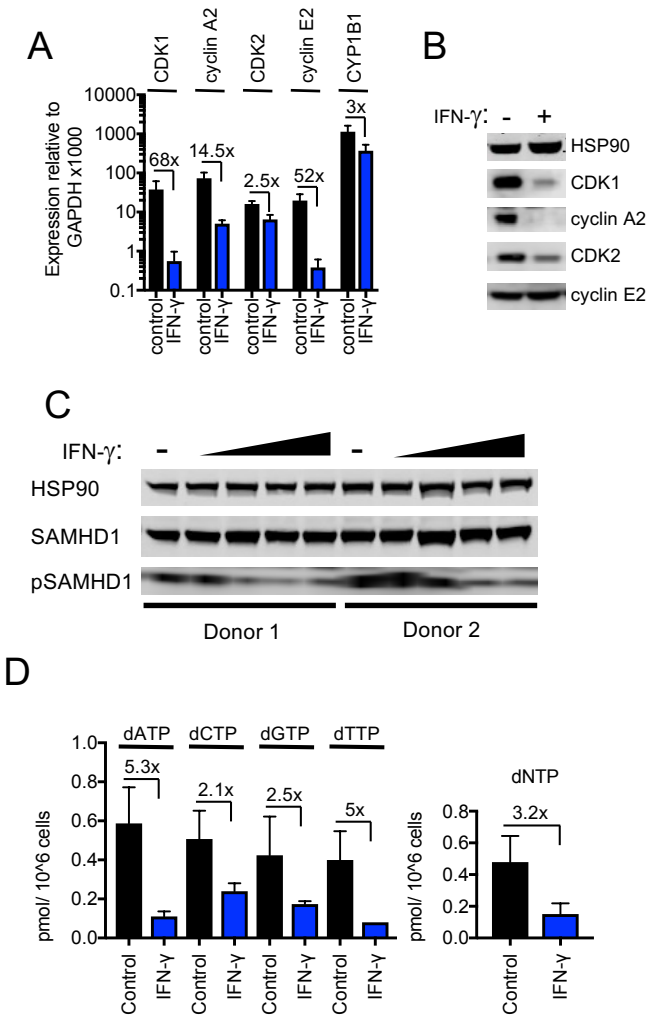

Figure 5: IFN-γ-mediated inhibition of viral replications is mechanistically similar to AhR

(A) Quantitative PCR analysis of CDK1, cyclin A2, CDK2, cyclin E2 and CYP1B1 mRNA levels in macrophages that were untreated or treated with IFN-γ. Numbers indicate fold-change, error bars represent standard deviation of data from 5 different donors.

(B) Western blot analysis of HSP90 (loading control) CDK1, cyclin A2, CDK2, cyclin E2 protein levels in macrophages treated with carrier (DMSO), AhR agonist or antagonist.

(C) Western blot analysis of HSP90 (loading control), total SAMHD1 levels, and phosphorylated SAMHD1 levels in macrophages treated with increasing concentrations of IFN-γ. Representative of 3 different donors.

(D) Analysis of dNTP levels in macrophages treated with IFN-γ. Error bars represent standard deviation of data from 3 different donors. Numbers indicate fold change.

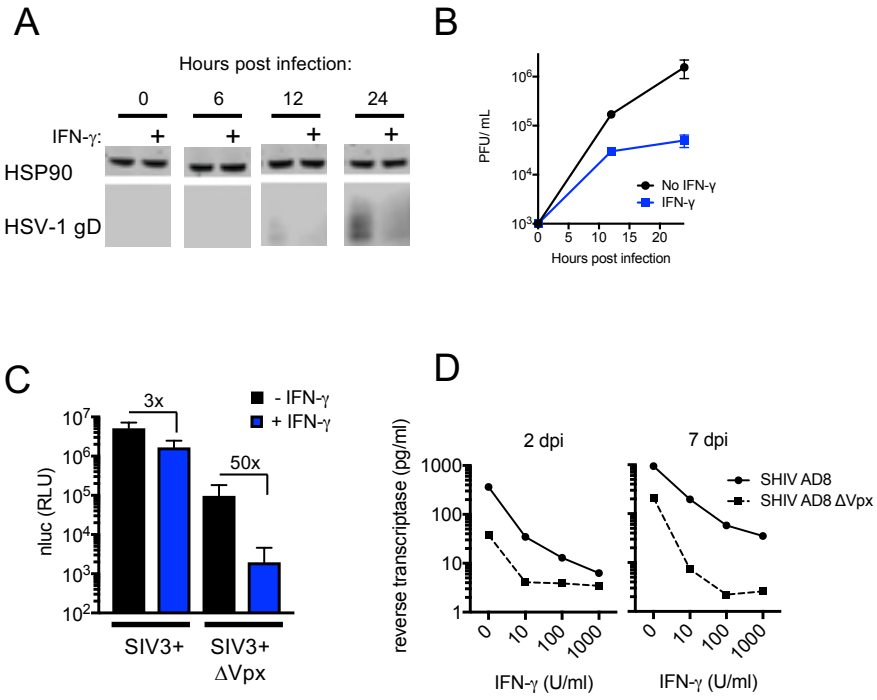

Figure 6: IFN-γ inhibits HIV-1 and HSV-1 replication, but SIV_{mac} Vpx confers resistance

(A) Western blot analysis of HSV-1 glycoprotein D (gD) over time in infected macrophages that were either untreated or treated with IFN-γ.

(B) HSV-1 infectious virion yield during replication in macrophages treated as in (A). Error bars represent standard deviation of two independent experiments.

(C) Single round infection in macrophages treated with SIV3+ or SIV3+ ΔVpx virus like particles and IFN-γ before infection with $HIV\text{-}1_{NLYU2}$-nluc. Numbers indicate fold change. Error bars represent standard deviation of data from 3 different donors.

(D) SHIV AD8 and SHIV AD8 ΔVpx reverse transcriptase levels in infected macrophages treated with increasing concentrations of IFN-γ. Error bars represent standard deviation of data 3 technical replicates, representative of 2 experiments.

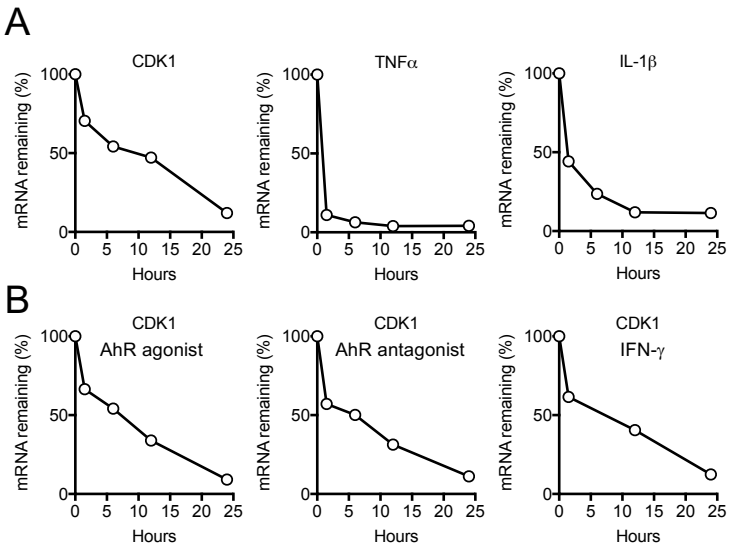

Figure 7: CDK1 mRNA stability is not affected by AhR and IFN-γ

(A) Decay rate of TNFα and IL-1β were monitored over time by qPCR and normalized to GAPDH. Representative example from three different donors.

(B) Transcriptional blockage with actinomycin D in the presence of AhR agonist, antagonist or IFN-γ. Decay rate of CDK1 was monitored over time by qPCR and normalized to GAPDH. Representative example from three different donors.

SUPPLEMENTAL INFORMATION

Supplemental figures

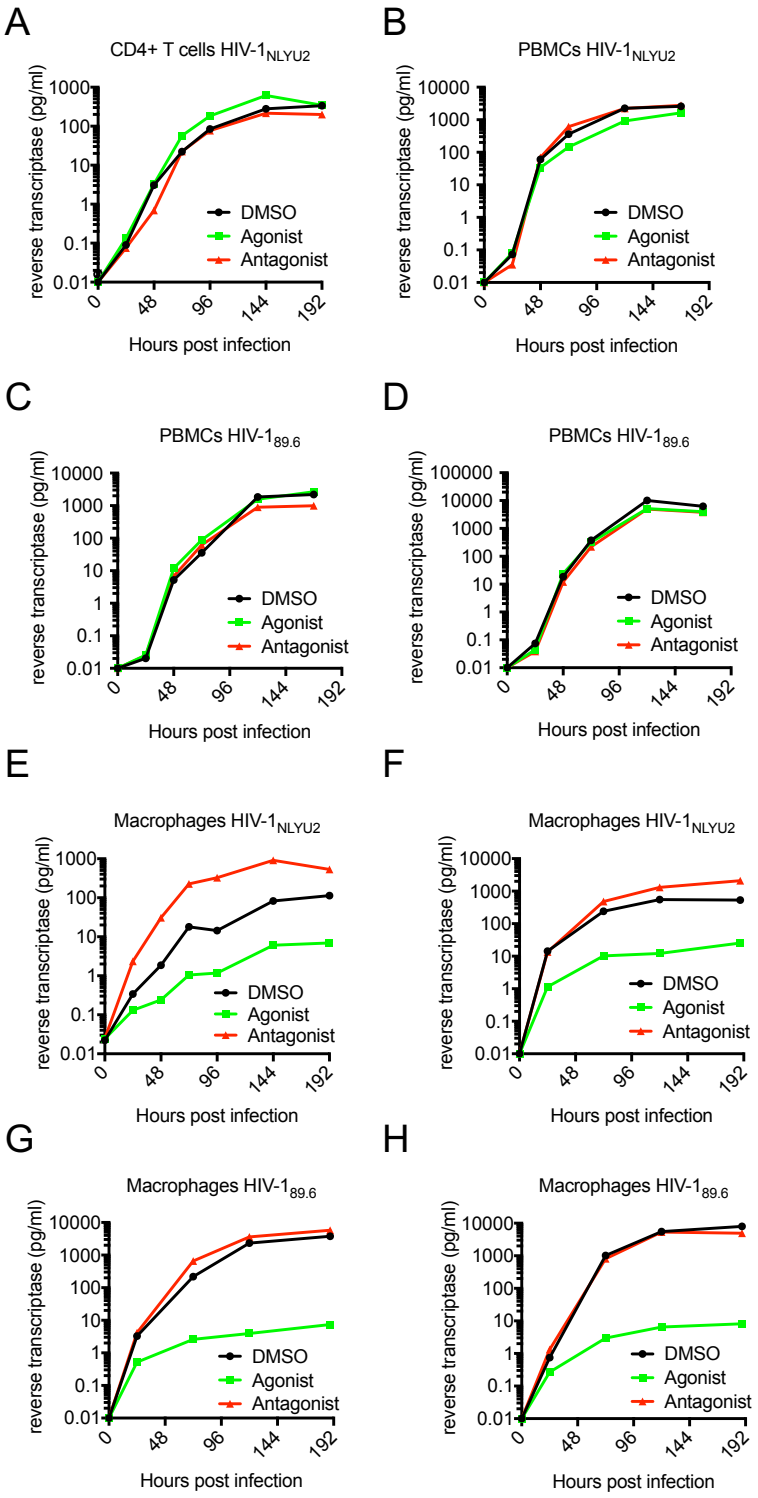

Figure 1-figure supplement 1. Effect of AhR activation on HIV-1 replication

(A – H) HIV-1 replication in CD4+ T cells (A) PBMCs (B-D) or macrophages (E-H), using strain HIV-$1_{NL\text{-}YU2}$ or HIV-$1_{89.6}$, as indicated.

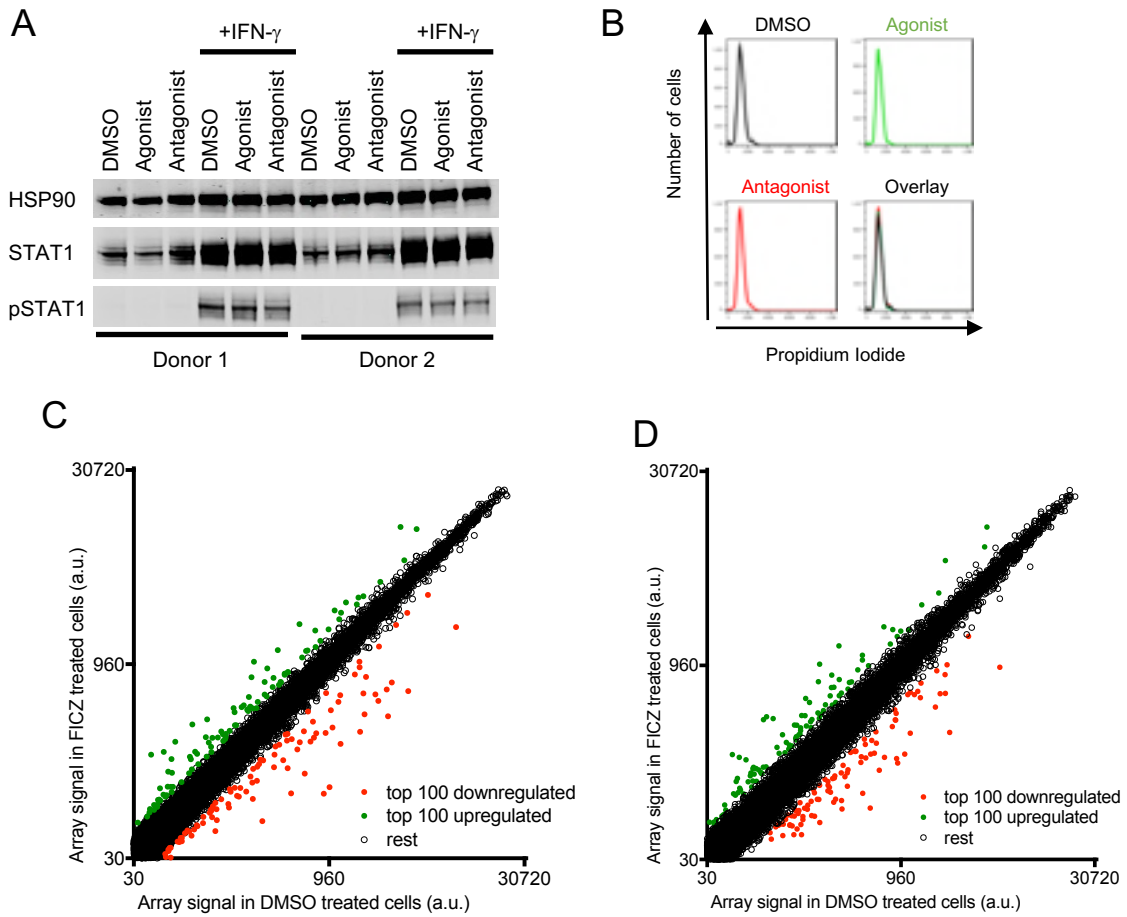

Figure 1-figure supplement 2. Effect of AhR activation on STAT1, cell-cycle and gene expression in macrophages

(A) Western blot analysis of STAT1 and phosphorylated STAT1 protein levels in macrophages treated with AhR agonist or antagonist and IFN-γ.

(B) FACS analysis of macrophages stained with propidium iodide to reveal DNA content distribution following treatment with the AhR agonist or antagonist. Representative of 3 different donors.

(C and D) Additional examples of microarray analysis of RNA extracted from macrophages from 2 different donors treated with AhR agonist or control. The array signal is plotted in arbitrary units (a.u.).

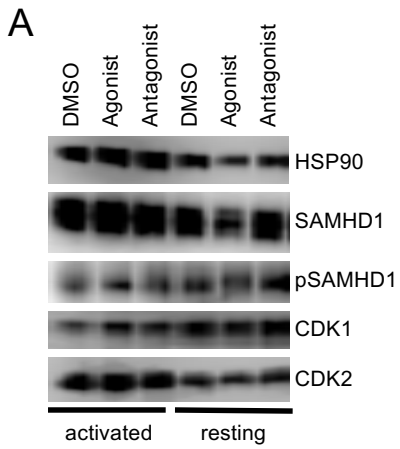

Figure 2-figure supplement 1. Effects of AhR activation in PBMC

(A) Protein levels of SAMHD1, phosphorylated SAMHD1, CDK1 and CDK2 in activated or resting PBMCs treated with carrier, AhR agonist or antagonist.

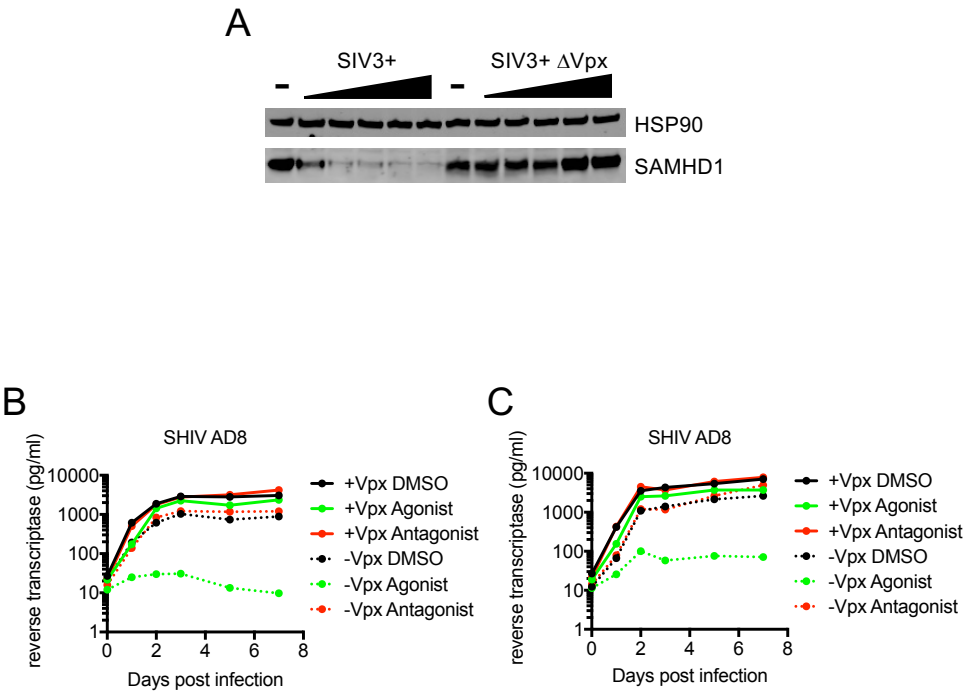

Figure 3-figure supplement 1. Vpx-induced degradation of SAMHD1 abolishes AhR-mediated inhibition in macrophages

(A) Western blot analysis of SAMHD1 and phosphorylated SAMHD1 in macrophages treated with increasing concentrations of SIV3+ or SIV3+ ΔVpx virus like particles.

(B and C) Virus replication assays in macrophages, from two different donors, treated with AhR agonist or antagonist and infected with chimeric SHIV AD8 virus expressing or not expressing the Vpx protein.

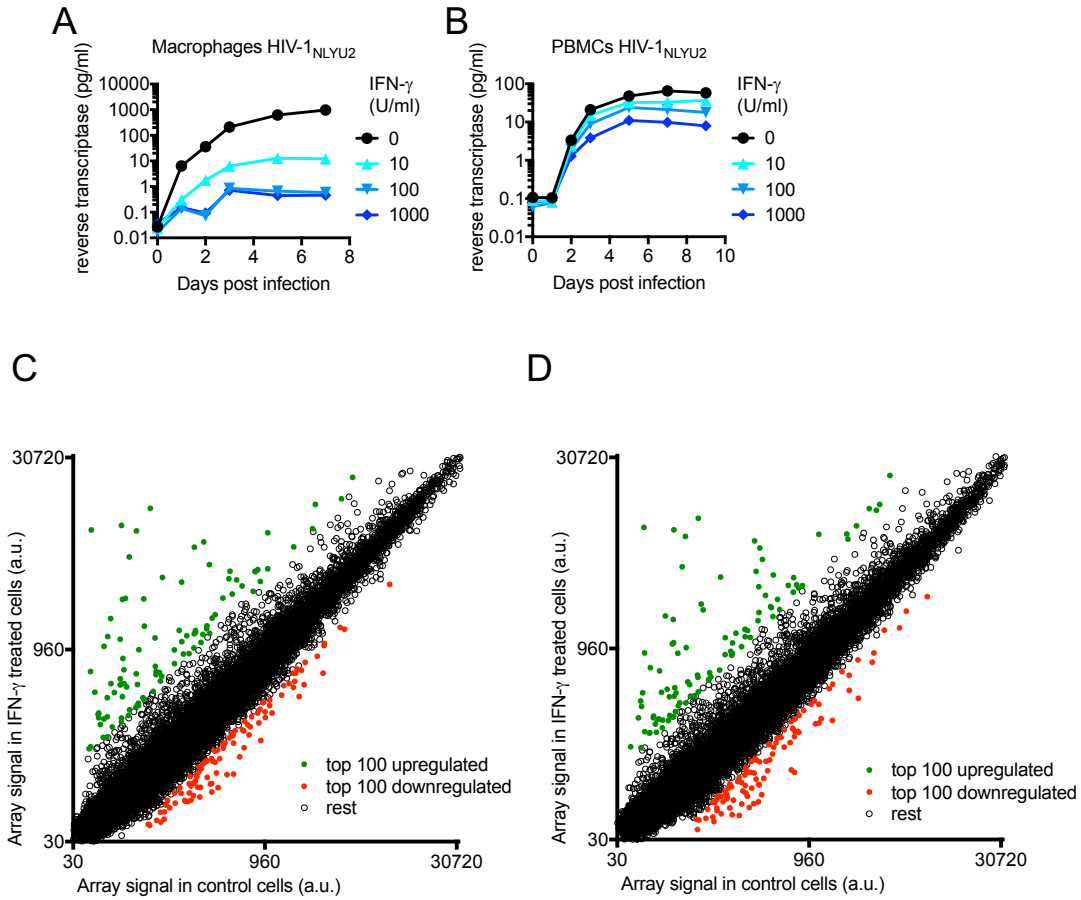

Figure 4-figure supplement 1. Effect of IFN-γ on HIV-1 replication and microarray analysis of IFN-γ-induced changes in mRNA levels

(A and B) HIV-1_{NL-YU2} replication in macrophages or PBMCs treated with increasing concentrations of IFN-γ.

(C and D) Microarray analysis of RNA extracted from macrophages, from two different donors, treated with IFN-γ or control. The array signal is plotted in arbitrary units (a.u.).

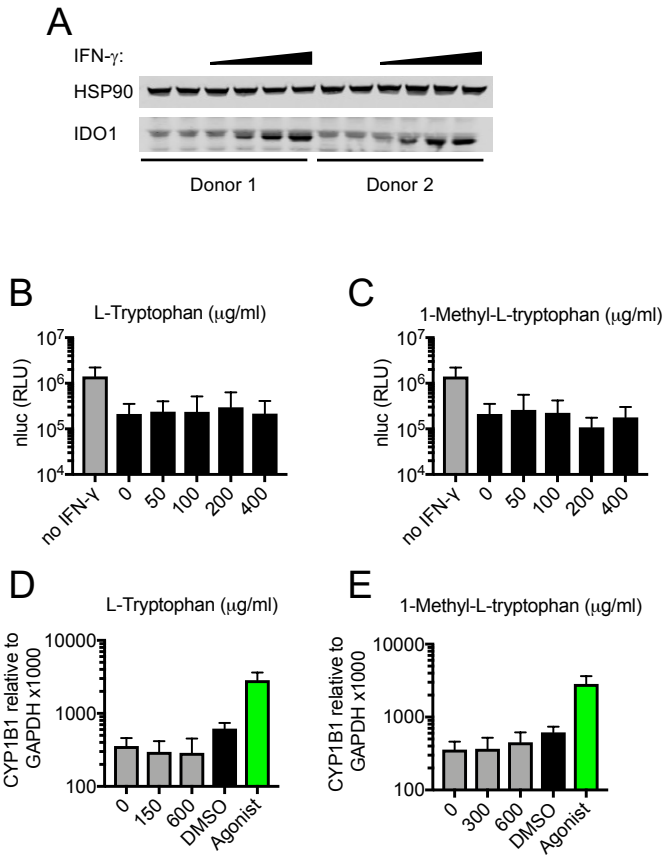

Figure 4-figure supplement 2. IDO1-mediated Tryptophan catabolism does not mediate the IFN-γ induced replication block

(A) Western blot analysis of HSP90 (loading control) and IDO1 expression in IFN-γ treated macrophages.

(B, C) Single round infection in macrophages treated with increasing concentrations of L-Tryptophan (B), 1-Methyl-L-tryptophan (C) respectively, and treated with 10 U/ml IFN-γ before infection with HIV-1_{NL-YU2}-nluc. Error bars represent standard deviation of data from two different donors.

(D, E) Quantitative PCR analysis of CYP1B1 in aforementioned macrophages treated with L-Tryptophan (D), 1-Methyl-L-tryptophan (E) and 10 U/ml IFN-γ. Error bars represent standard deviation of data from two different donors.

Supplemental tables

Donor 1		Donor 2		Donor 3	
Gene:	Fold change	Gene:	Fold change	Gene:	Fold change
SEMA6B	5.85	THBS1	4.68	SEMA6B	4.43
RASAL1	5.74	GPR68	3.96	CYGB	4.41
GPR68	4.84	RASAL1	3.93	TNFAIP8L3	4.38
IL1B	4.15	SEMA6B	3.86	GPR68	4.29
XYLT1	4.06	SRPX	3.84	RASAL1	4.15
FUCA1	4.02	EBI2	3.46	IL1B	3.80
NCF1	3.93	CYP1B1	3.26	CXCR5	3.49
TMEM119	3.88	TMEM119	3.25	EBI2	3.27
THBS1	3.87	TIPARP	3.19	ITGB7	3.05
TIPARP	3.66	XYLT1	3.13	COL23A1	2.96
EBI2	3.58	LRP5	3.01	FUCA1	2.94
TNFAIP8L3	3.44	CYGB	2.77	TIPARP	2.91
NCF1C	3.33	HS.434957	2.55	IL8	2.71
LOC645638	3.24	ABCC4	2.49	NCF1C	2.65
THBD	3.16	TNFAIP8L3	2.42	CYP1B1	2.54
CYGB	3.03	INSIG1	2.37	F13A1	2.48
ADORA3	2.92	FUCA1	2.36	GREM1	2.41
COL23A1	2.88	PRDM8	2.34	SLC16A6	2.41
QPRT	2.76	ADK	2.33	THBD	2.40
LOC652616	2.76	GFRA2	2.31	PHLDA1	2.39
PHLDA1	2.74	PHLDA1	2.29	NCF1	2.34
CXCR5	2.67	PTGFRN	2.27	COLEC12	2.33
CYP1B1	2.54	COL23A1	2.27	KCNF1	2.32
GREM1	2.51	GPR183	2.25	TMEM119	2.27
SLC16A6	2.43	F13A1	2.23	STAB1	2.26
ITGB7	2.41	QPRT	2.19	RAP1GAP	2.25
GPR183	2.34	GAPT	2.19	M160	2.23
RAP1GAP	2.30	ADORA3	2.18	HSPE1	2.21
INSIG1	2.28	ITGB7	2.13	RNASE1	2.20
GCNT1	2.24	COBLL1	2.13	ADK	2.20
ABHD12	2.22	NCF4	2.10	TCTEX1D1	2.14
ADK	2.22	SLC16A6	2.10	CAMK2B	2.13
M160	2.21	NT5DC2	2.08	GPR183	2.12
LPAR2	2.20	ABI3	2.04	ABHD12	2.06
RUNX3	2.18	EPB41L3	2.03	COLQ	2.06
MEF2A	2.15	ABCB4	1.97	PTPN6	2.03
C13ORF31	2.14	M160	1.95	ABCB4	2.01
CD163L1	2.11	LOC731658	1.95	SLC26A11	2.00
ABI3	2.11	RAP1GAP	1.94	CCL1	1.99
PTPN6	2.10	CD163L1	1.91	LOC728755	1.98
CADM1	2.10	CHN2	1.90	LOC645638	1.98
TNFSF14	2.08	SLC1A5	1.90	ADORA3	1.97
NOTCH1	2.05	ADORA2B	1.88	NT5DC2	1.96
CD226	2.03	GCNT1	1.88	CD226	1.93
IL8	2.00	PMP22	1.88	CADM1	1.92
MAOA	2.00	RASSF2	1.87	ATP8B4	1.91
CAMK2B	1.99	PTPN6	1.87	HS.197143	1.91
PSTPIP2	1.99	NBL1	1.86	LOC100128274	1.91
PDPN	1.99	HBEGF	1.86	ISYNA1	1.90
ISYNA1	1.98	CCM2	1.85	CD163L1	1.89
HK2	1.98	IL1B	1.85	NISCH	1.89
GPR162	1.97	TFAP2C	1.84	PTGFRN	1.88
MAFF	1.97	IL18BP	1.83	SAMSN1	1.87
C3ORF59	1.96	RUNX3	1.83	TEX12	1.87
C14ORF43	1.95	NISCH	1.82	CDKN1A	1.86
NCF4	1.95	RNASE1	1.82	IL18BP	1.86
KIAA1671	1.94	IGF1	1.82	INSIG1	1.85
PTGFRN	1.92	BTG2	1.82	TNFSF14	1.85
TCTEX1D1	1.90	ABHD12	1.81	PTGS2	1.84
P2RY5	1.89	AKAP11	1.81	GCNT1	1.84
HBEGF	1.88	LOC727970	1.81	C19ORF59	1.84
NISCH	1.87	NCF1	1.81	LOC727962	1.82
IRF5	1.86	BEX1	1.81	ZNF395	1.82
CCM2	1.86	DMXL1	1.80	LOC652616	1.82
GAPT	1.84	IL8	1.80	HBEGF	1.80
IER3	1.84	HS.532698	1.79	PDGFRA	1.80
TMEM45B	1.82	C10ORF105	1.79	SLC2A3	1.80
MAPK8IP2	1.82	HS.458448	1.78	SLC25A24	1.79
PLEKHF1	1.82	FCGR2B	1.78	CDK5RAP2	1.78
IL18BP	1.81	C20ORF3	1.77	RBM38	1.78
LOC653820	1.81	LOC441759	1.76	PSTPIP2	1.78
CDKN1A	1.80	RPL8	1.75	C8ORF45	1.77
F13A1	1.80	MAFF	1.75	LMOD3	1.77
TRIM54	1.79	LOC283663	1.75	NQO1	1.77
FCRLA	1.78	HOXA5	1.75	RAB38	1.77
NQO1	1.77	HSPE1	1.75	JARID2	1.77
EPB41L3	1.76	UBE2U	1.73	HSPA5	1.76
CYBASC3	1.76	P2RY5	1.73	HOXA5	1.76
STOX2	1.76	PDGFB	1.73	ATP2A3	1.74
MSC	1.76	SAP30	1.72	ABI3	1.74
EPHB2	1.76	THBD	1.72	LOC100131390	1.73
MIDN	1.76	HS.291377	1.72	TFAP2C	1.73
ANXA11	1.75	ARMC9	1.71	RPL10	1.72
CD93	1.75	RGS10	1.71	SLC9A9	1.72
IRF2BP2	1.75	ETS2	1.71	LOC100129882	1.69
SAMSN1	1.73	C14ORF43	1.70	C20ORF123	1.69
NBL1	1.73	OLR1	1.70	TACC2	1.68
SH3PXD2B	1.73	APBB3	1.70	EPHB2	1.68
ATP8B4	1.72	TACC2	1.68	NCF4	1.68
KLF13	1.70	CDKN1A	1.68	ITGA11	1.67
NINJ1	1.70	RAB38	1.68	FAM73A	1.67
GPR82	1.70	RBP1	1.68	METRNL	1.67
TACC2	1.69	ARL4C	1.67	SRPX	1.67
BTG2	1.69	ITGA9	1.66	GCLC	1.67
BHLHB3	1.69	CAMK2B	1.66	MAFF	1.66
SEPP1	1.68	LOC652424	1.66	HS.564097	1.66
C10ORF105	1.68	PDK4	1.66	C3ORF59	1.65
LOC100133234	1.68	GIYD2	1.66	SNAPC1	1.64
RIN1	1.68	NCF1C	1.65	ALOX5	1.64
GCLC	1.67	TMEM26	1.65	LOC440015	1.64

Table S1. Top 100 upregulated genes in AhR activated macrophages. The fold change in mRNA levels, relative to carrier treated cells, for the top 100 AhR-activation-induced genes is given.

Donor 1		Donor 2		Donor 3	
Gene:	Fold change	Gene:	Fold change	Gene:	Fold change
CXCL10	0.21	IFI44L	0.11	IFIT1	0.13
CDC45L	0.28	CXCL10	0.11	IFI44L	0.14
TYMS	0.28	IFIT2	0.14	MX1	0.16
IFIT1	0.29	IFIT1	0.15	HERC5	0.19
GINS2	0.31	IFIT3	0.17	IFIT2	0.19
MCM7	0.31	RSAD2	0.20	RSAD2	0.20
IFIT2	0.32	MX2	0.20	MX2	0.20
NCAPG	0.33	OASL	0.20	CXCL10	0.22
HERC5	0.33	MX1	0.20	IFIT3	0.23
KIAA0101	0.33	ISG15	0.22	EPSTI1	0.25
TOP2A	0.33	HERC5	0.22	OAS2	0.26
IFI44L	0.33	CCL8	0.22	CDC45L	0.26
E2F2	0.34	OAS2	0.23	UHRF1	0.26
CDC20	0.34	EPSTI1	0.24	MCM7	0.26
UHRF1	0.35	IFI44	0.26	IFI44	0.27
HS.545589	0.35	OAS3	0.30	HS.545589	0.29
CDCA5	0.35	PRIC285	0.31	E2F2	0.29
MARCKS	0.35	STAT1	0.32	CCNE2	0.30
CCNA2	0.36	XAF1	0.33	ISG15	0.30
EXO1	0.36	IRF7	0.35	TYMS	0.30
HAMP	0.37	USP18	0.35	GINS2	0.32
UBE2C	0.37	SAMD9L	0.35	RNU6ATAC	0.33
CCNE2	0.38	OAS1	0.37	PARP14	0.34
CEP55	0.38	CXCL11	0.38	KIAA0101	0.34
RAD51AP1	0.38	PARP9	0.38	NCAPG	0.35
NEXN	0.38	GBP1	0.41	MCM10	0.35
CDC2	0.38	EIF2AK2	0.41	OAS1	0.35
IFIT3	0.39	HERC6	0.42	OAS3	0.36
PLK4	0.39	TNFSF10	0.42	C11ORF82	0.36
USP18	0.39	SP110	0.43	MAD2L1	0.37
MCM10	0.39	IFI35	0.43	OASL	0.37
CDT1	0.39	GBP5	0.45	MCM4	0.37
HSPE1	0.39	IL4I1	0.45	P2RX7	0.38
MX1	0.40	ISG20	0.45	LOC100008589	0.39
CCL8	0.40	IFI27	0.46	PRIC285	0.39
PRC1	0.40	DDX58	0.47	PRC1	0.39
IFI44	0.40	GBP4	0.47	PARP9	0.39
HMMR	0.41	IFIH1	0.47	PRIM1	0.39
TMEM97	0.41	PARP14	0.47	EXO1	0.40
C11ORF82	0.41	SAMD9	0.48	CDCA5	0.40
NDC80	0.41	SDS	0.49	STAT1	0.40
CENPM	0.41	AIM2	0.49	IRF7	0.40
MCM4	0.41	HAMP	0.51	CDCA7	0.40
GAL3ST4	0.41	HESX1	0.52	TRIM22	0.40
KIFC1	0.41	P2RX7	0.52	DDX60	0.41
TMEM106C	0.42	LOC730099	0.53	USP18	0.41
LOC100133005	0.42	IFITM2	0.53	CEP55	0.41
MX2	0.42	TNFAIP6	0.53	GBP1	0.41
ANLN	0.43	CDC45L	0.54	ISG20	0.42
PPAP2B	0.43	TRIM22	0.54	SP110	0.42
RNU6ATAC	0.43	TRIM5	0.54	POLE2	0.42
EPSTI1	0.43	PDGFRL	0.55	XAF1	0.43
CCL4L1	0.43	IFITM3	0.55	IL4I1	0.43
MCM6	0.43	PLSCR1	0.55	TNFSF10	0.44
MELK	0.44	STAT2	0.57	CCNA2	0.44
TK1	0.44	CXCL2	0.57	MCM2	0.44
OASL	0.45	HS.125087	0.57	SAMD9L	0.44
DNAJC9	0.45	CMPK2	0.57	HAMP	0.44
OIP5	0.45	SOD2	0.57	IFI6	0.44
FBXO5	0.45	DHX58	0.58	ATAD2	0.45
MCM2	0.45	FBXO7	0.58	TMEM97	0.45
SPC25	0.46	LOC643194	0.58	HERC6	0.45
HELLS	0.46	DDX60L	0.58	CDT1	0.46
HIST1H4C	0.46	FAM26F	0.58	PLK4	0.46
FEN1	0.46	RN5S9	0.59	MT1X	0.46
TRIP13	0.46	CXCL9	0.59	SIGLEC14	0.46
KIF11	0.46	LOC400759	0.59	CDC2	0.46
CKAP2L	0.46	GAL3ST4	0.59	MELK	0.46
CCNB2	0.47	DDX60	0.59	EIF2AK2	0.46
PRIM1	0.47	TOR1B	0.60	MARCKS	0.47
CCL3L1	0.47	LOC646034	0.60	RAD51AP1	0.47
PLSCR1	0.47	CCL13	0.60	TNFSF13B	0.48
MAD2L1	0.48	CD80	0.60	FEN1	0.48
ASPM	0.48	C11ORF82	0.60	UBE2C	0.48
AURKB	0.48	HS.62927	0.61	MPP6	0.48
CCL3L3	0.48	UHRF1	0.61	GBP5	0.48
BUB1	0.48	FAM19A3	0.61	SAMD9	0.48
POLE2	0.49	CCNE2	0.61	RFC4	0.49
DLGAP5	0.49	VCAM1	0.61	PFKM	0.49
DEPDC1	0.49	TNFSF13B	0.61	CCRL2	0.50
GMNN	0.49	UBE2L6	0.61	IL1RN	0.50
C16ORF75	0.50	TYMS	0.61	TTK	0.50
CCL3	0.50	MCM10	0.62	C3ORF26	0.50
STIL	0.50	MRGPRG	0.62	MSH6	0.51
LOC728835	0.50	JUP	0.62	PPAP2B	0.51
NUSAP1	0.50	CLK2P	0.62	MT2A	0.51
UNG	0.50	SYNM	0.62	SDS	0.51
PRIC285	0.51	HRASLS3	0.62	KIF11	0.51
CHAF1B	0.51	IL1RN	0.62	BUB1	0.51
UBE2T	0.51	IFITM1	0.62	MYC	0.52
STMN1	0.51	LAP3	0.63	CENPM	0.52
CDC25A	0.51	DDEF2	0.63	TIMELESS	0.52
TTK	0.51	LOC100133005	0.63	MCM5	0.52
PCNA	0.52	ARHGEF15	0.63	TK1	0.52
LOC729816	0.52	NT5C3	0.63	KIFC1	0.52
SIGLEC14	0.52	SOX2	0.63	SNCA	0.52
CCL4L2	0.52	HS.545589	0.63	MCM6	0.52
CHEK1	0.52	ZC3HAV1	0.63	POLQ	0.52
RFC4	0.52	GINS2	0.64	CHAF1B	0.52
SP110	0.52	LOC401914	0.64	CCL7	0.53

Table S2. Top 100 downregulated genes in AhR activated macrophages. The fold change in mRNA levels, relative to carrier treated cells, for the top 100 AhR-activation-repressed genes is given.

A

Pathway name	#Entities found	Submitted entities found
Immune System	59	IFITM3;IFITM1;IL1RN;IFITM2;TNFAIP6;CD80;UBE2L6;KIF11;IFI35;IFIT1;CXCL2;IFIT3;IFIT2;OASL;TNFSF13B;SOX2;IFIH1;HERC5;CDC20;MT2A;TRIM5;MYC; DHX58;FBXO7;TRIM22;HERC6;GBP5;RSAD2;DDX58;SP110;AIM2;OAS1;IFI27;OAS2;OAS3;IRF7;LAP3;CCL3L1;CCL3L3;IFI6;USP18;CCL3;GBP1;GBP4;VCAM1; SIGLEC14;JUP;STAT1;UBE2C;STAT2;MX2;MX1;EIF2AK2;ISG15;SOD2;ISG20;P2RX7;CXCL10;XAF1
Cytokine Signaling in Immune system	47	IFITM3;IFITM1;IL1RN;IFITM2;CCL3L1;CCL3L3;CD80;IFI6;UBE2L6;IFI35;IFIT1;CXCL2;USP18;IFIT3;IFIT2;OASL;TNFSF13B;SOX2;HERC5;MT2A;TRIM5;MYC; CCL3;GBP1;GBP4;TRIM22;HERC6;GBP5;VCAM1;RSAD2;DDX58;STAT1;SP110;STAT2;MX2;MX1;EIF2AK2;ISG15;SOD2;ISG20;CXCL10;OAS1;IFI27;OAS2; OAS3;IRF7;XAF1
Cell Cycle	43	TOP2A;FEN1;PCNA;MCM7;CDCA5;PRIM1;GMNN;NCAPG;MCM10;HMMR;TYMS;AURKB;CDC20;CCNB2;EXO1;MYC;CHEK1;E2F2;OIP5;TK1;CDC45L;FBXO5; C16ORF75;BUB1;PLK4;CDT1;GINS2;RFC4;UBE2C;NDC80;CDC25A;CDC2;CCNA2;CCNE2;POLE2;CENPM;MCM4;MCM5;MCM6;HIST1H4C;SPC25;MAD2L1; MCM2
Cell Cycle, Mitotic	39	TOP2A;FEN1;PCNA;MCM7;CDCA5;PRIM1;GMNN;NCAPG;MCM10;HMMR;TYMS;AURKB;CDC20;CCNB2;MYC;E2F2;TK1;CDC45L;FBXO5;BUB1;PLK4;CDT1; GINS2;RFC4;UBE2C;NDC80;CDC25A;CDC2;CCNA2;CCNE2;POLE2;CENPM;MCM4;MCM5;MCM6;HIST1H4C;SPC25;MAD2L1;MCM2
Interferon Signaling	36	IFITM3;IFITM1;IFITM2;IFI6;UBE2L6;IFI35;IFIT1;USP18;IFIT3;IFIT2;OASL;HERC5;MT2A;TRIM5;GBP1;GBP4;TRIM22;HERC6;GBP5;VCAM1;RSAD2;SP110; DDX58;STAT1;MX2;STAT2;MX1;EIF2AK2;ISG15;ISG20;OAS1;IFI27;OAS2;OAS3;IRF7;XAF1
Signal Transduction	27	CCL13;CXCL9;CCL4L1;CD80;CCL4L2;CXCL2;AURKB;SOX2;CDC20;MYC;CCRL2;CHEK1;TNFSF10;BUB1;DLGAP5;JUP;ARHGEF15;STAT1;NDC80;CDC2; CXCL10;CXCL11;PRC1;CENPM;HIST1H4C;SPC25;MAD2L1
Cell Cycle Checkpoints	25	MCM7;MCM10;AURKB;CDC20;CCNB2;EXO1;CHEK1;CDC45L;C16ORF75;BUB1;RFC4;UBE2C;NDC80;CDC25A;CDC2;CCNA2;CCNE2;CENPM;MCM4;MCM5; MCM6;HIST1H4C;SPC25;MAD2L1;MCM2
Interferon alpha/beta signaling	23	IFITM3;IFITM1;IFITM2;RSAD2;STAT1;MX2;STAT2;MX1;IFI6;ISG15;IFI35;IFIT1;USP18;IFIT3;IFIT2;OASL;ISG20;OAS1;IFI27;OAS2;OAS3;IRF7;XAF1
Mitotic G1-G1/S phases	21	TOP2A;CDT1;PCNA;MCM7;PRIM1;MCM10;TYMS;CDC25A;CDC2;CCNA2;CCNE2;MYC;POLE2;E2F2;MCM4;MCM5;TK1;CDC45L;MCM6;FBXO5;MCM2
Metabolism of proteins	20	TOP2A;PCNA;UBE2C;SP110;DDX58;UBE2L6;USP18;AURKB;CDC25A;CDC2;IFIH1;CDC20;CCNA2;CCNE2;MYC;UBE2T;HIST1H4C;FBXO7;SPC25;SNCA
G1/S Transition	19	CDT1;PCNA;MCM7;PRIM1;MCM10;TYMS;CDC25A;CDC2;CCNA2;CCNE2;MYC;POLE2;MCM4;MCM5;TK1;CDC45L;MCM6;FBXO5;MCM2
S Phase	19	CDT1;GINS2;FEN1;PCNA;RFC4;MCM7;PRIM1;CDCA5;CDC25A;CDC2;CCNA2;CCNE2;MYC;POLE2;MCM4;MCM5;CDC45L;MCM6;MCM2
DNA Repair	19	POLQ;FEN1;PCNA;RFC4;UBE2L6;ISG15;CDC2;UNG;MSH6;RAD51AP1;CCNA2;KIAA0101;EXO1;POLE2;UBE2T;CHEK1;TIMELESS;HIST1H4C;C16ORF75
DNA Replication	18	CDT1;GINS2;FEN1;PCNA;RFC4;MCM7;PRIM1;GMNN;MCM10;CDC2;CCNA2;POLE2;E2F2;MCM4;MCM5;CDC45L;MCM6;MCM2
Post-translational protein modification	16	TOP2A;PCNA;UBE2C;SP110;DDX58;USP18;AURKB;CDC25A;CDC2;IFIH1;CDC20;CCNA2;MYC;UBE2T;HIST1H4C;FBXO7
Metabolism	16	FEN1;HMMR;TYMS;PARP9;PARP14;HSPE1;NT5C3;CDC2;PRIC285;IL4I1;MARCKS;AIM2;PPAP2B;HRASLS3;TK1;PFKM
Gene expression (Transcription)	15	PCNA;RFC4;UHRF1;STAT1;ATAD2;AURKB;CDC2;PRIC285;CCNA2;CCNE2;EXO1;MYC;CHEK1;HIST1H4C;C16ORF75
Synthesis of DNA	15	CDT1;GINS2;FEN1;PCNA;RFC4;MCM7;PRIM1;CDC2;CCNA2;POLE2;MCM4;MCM5;CDC45L;MCM6;MCM2
G2/M Checkpoints	15	RFC4;MCM7;MCM10;CDC25A;CDC2;CCNB2;EXO1;CHEK1;MCM4;MCM5;CDC45L;MCM6;HIST1H4C;C16ORF75;MCM2
M Phase	15	PLK4;UBE2C;CDCA5;NCAPG;AURKB;NDC80;CDC2;CDC20;CCNB2;CENPM;FBXO5;HIST1H4C;BUB1;SPC25;MAD2L1

B

Pathway name	#Entities found	Submitted entities found
Cell Cycle	30	TOP2A;MCM7;CDCA5;NCAPG;MCM10;HMMR;TYMS;CDC20;CCNB2;CCNB1;CCND2;EXO1;CEP70;E2F2;OIP5;NEK2;TK1;CDC45L;BUB1;GINS2;CDKN2B;UBE2C;CDC2;CCN A2;CCNE2;CENPM;MCM4;HIST1H4C;MAD2L1;MCM2
Signal Transduction	30	RGS18;NOTCH3;EBI2;PDE3B;FAM13A;CXCR5;CXCR4;LPL;LFNG;CDC20;RGS2;NCK2;PDK4;MYH10;BUB1;DLGAP5;CDKN2B;OPN3;VWF;ITGA3;USP2;AKR1C3;CDC2;PRC1; GPER;CENPM;SDC1;UTS2;HIST1H4C;MAD2L1
Cell Cycle, Mitotic	28	TOP2A;MCM7;CDCA5;NCAPG;MCM10;HMMR;TYMS;CDC20;CCNB2;CCNB1;CCND2;CEP70;E2F2;NEK2;TK1;CDC45L;BUB1;GINS2;CDKN2B;UBE2C;CDC2;CCNA2;CCNE2; CENPM;MCM4;HIST1H4C;MAD2L1;MCM2
Metabolism	22	PNPLA7;CERK;ABCC5;AKR1C3;LPL;XYLT1;C7ORF68;HMMR;TYMS;BRI3BP;CDC2;NUDT7;AMDHD1;ALOX5AP;GPD1;PDK4;ACOT2;SMS;ITGB1BP3;SDC1;TK1;TNFRSF21
Immune System	20	COLEC12;ATP8B4;TNFSF14;CLEC12A;UBE2C;KIF11;RAP1GAP;CDC20;SYNGR1;FSCN1;CD300LB;SDC1;OLR1;METTL7A;CD14;TLR5;AMICA1;CAMP;C19ORF59;HSPA1A
Cell Cycle Checkpoints	17	MCM7;UBE2C;MCM10;CDC2;CDC20;CCNA2;CCNB2;CCNB1;CCNE2;EXO1;CENPM;MCM4;CDC45L;HIST1H4C;BUB1;MAD2L1;MCM2
Mitotic G1-G1/S phases	15	TOP2A;CDKN2B;MCM7;MCM10;TYMS;CDC2;CCNA2;CCNB1;CCND2;CCNE2;E2F2;MCM4;CDC45L;TK1;MCM2
Gene expression (Transcription)	14	BNIP3L;NOTCH3;CDKN2B;GADD45A;USP2;TDRD9;CDC2;CCNA2;CCNB1;CCND2;CCNE2;EXO1;HIST1H4C;PHF19
M Phase	13	UBE2C;CDCA5;NCAPG;CDC2;CDC20;CCNB2;CCNB1;CEP70;CENPM;NEK2;HIST1H4C;BUB1;MAD2L1
Generic Transcription Pathway	12	CCNA2;BNIP3L;NOTCH3;CDKN2B;CCNB1;CCND2;CCNE2;EXO1;GADD45A;USP2;HIST1H4C;CDC2
RNA Polymerase II Transcription	12	CCNA2;BNIP3L;NOTCH3;CDKN2B;CCNB1;CCND2;CCNE2;EXO1;GADD45A;USP2;HIST1H4C;CDC2
GPCR downstream signaling	12	RGS18;RGS2;OPN3;EBI2;PDE3B;GPER;CXCR5;AKR1C3;SDC1;CXCR4;UTS2;LPL
Signaling by GPCR	12	RGS18;RGS2;OPN3;EBI2;PDE3B;GPER;CXCR5;AKR1C3;SDC1;CXCR4;UTS2;LPL
G1/S Transition	11	CCNA2;CCNB1;MCM7;CCNE2;MCM4;MCM10;CDC45L;TK1;TYMS;MCM2;CDC2
Mitotic Prometaphase	11	CDC20;CCNB2;CCNB1;CDCA5;CEP70;NCAPG;CENPM;NEK2;BUB1;CDC2;MAD2L1
Innate Immune System	11	SYNGR1;ATP8B4;CLEC12A;CD300LB;OLR1;METTL7A;CD14;TLR5;CAMP;C19ORF59;HSPA1A
Metabolism of lipids	10	NUDT7;CERK;PNPLA7;GPD1;ALOX5AP;ACOT2;AKR1C3;C7ORF68;BRI3BP;TNFRSF21
G2/M Checkpoints	10	CCNB2;CCNB1;MCM7;EXO1;MCM4;MCM10;CDC45L;HIST1H4C;CDC2;MCM2
Hemostasis	10	SPARC;VWF;ITGA3;PDE3B;SDC1;OLR1;TIMP3;KIF11;AMICA1;TFPI
Metabolism of proteins	10	CDC20;TOP2A;CCNA2;CCNE2;UBE2C;UBE2T;USP2;HIST1H4C;CDC2;DCAF6

Table S3. Pathway analysis of top 100 downregulated genes in AhR activated (A)

and IFN-γ stimulated (B) macrophages

Donor 1		Donor 2		Donor 3	
Gene:	Fold change	Gene:	Fold change	Gene:	Fold change
IDO1	159.03	IDO1	176.73	IDO1	255.33
CCL8	98.62	CCL8	125.66	RARRES3	115.25
GBP5	78.49	GBP5	101.39	GBP5	73.91
RARRES3	71.29	RARRES3	86.82	GBP4	73.22
GBP4	43.61	GBP4	61.94	CCL8	71.87
GPBAR1	24.17	GPBAR1	32.53	GPBAR1	33.08
AIM2	19.67	AIM2	31.30	GBP1	31.98
GBP1	18.82	ANKRD22	28.44	LOC400759	26.51
ANKRD22	18.07	LOC400759	23.46	ISG20	26.17
LOC400759	18.05	VAMP5	22.69	FAM26F	24.00
FAM26F	15.75	RSAD2	22.31	AIM2	22.77
VAMP5	15.09	ISG20	21.65	RSAD2	19.38
RSAD2	13.69	GBP1	21.08	ANKRD22	17.77
ISG20	12.87	CXCL10	19.41	IL27	16.58
SERPING1	12.84	SERPING1	16.52	CCL2	16.27
CXCL10	12.42	CXCL9	15.71	IRF1	15.51
IRF1	11.68	CCL2	15.20	SERPING1	13.93
CCL2	10.54	FAM26F	13.49	VAMP5	13.68
GCH1	9.92	IRF1	12.66	EPSTI1	12.22
ASCL2	9.83	ASCL2	11.11	ASCL2	12.01
APOL3	9.35	IL27	10.03	IFI44L	11.90
IL27	9.06	APOL3	9.73	BRDG1	11.57
CXCL9	8.09	CCL7	8.99	GCH1	11.47
IFIT2	7.61	STAP1	8.87	NCF1	11.27
EPSTI1	7.24	GCH1	8.73	TYMP	11.23
CIITA	7.22	IFI27	8.06	LOC100133678	11.14
GBP2	6.66	GBP2	7.82	APOL3	10.73
IFI44L	6.51	SOD2	7.72	IL18BP	10.55
UBD	6.20	TNFSF10	7.25	IFITM3	10.15
STAP1	6.20	HLA-DOA	7.22	STAP1	9.68
IFIT3	5.77	MGC33556	7.20	HLA-DQA1	9.47
CD40	5.56	SOCS1	7.00	LOC100133583	9.19
FGL2	5.52	BRDG1	6.92	HLA-DOA	8.85
WARS	5.35	IFIT2	6.88	IL15	8.60
BRDG1	5.19	IFITM3	6.66	IFIT2	8.44
NCF1	4.97	IFI44L	6.61	TNFSF10	8.31
SOCS1	4.93	RSPO3	6.41	TNFSF13B	8.31
IL15	4.89	UBD	6.34	ITGB7	8.07
NFIX	4.86	ITK	6.22	WARS	7.65
STAMBPL1	4.83	HAPLN3	5.89	CIITA	7.52
STAT1	4.79	EPSTI1	5.88	CD40	7.13
TNFSF10	4.76	STAMBPL1	5.62	ECGF1	6.95
FCGR1B	4.75	TAP1	5.53	SOCS1	6.78
GIMAP8	4.64	IFIT3	5.42	IFIT3	6.76
FCGR1A	4.58	GIMAP8	5.35	STAT1	6.73
GK	4.52	IL15	5.34	LOC389386	6.63
C21ORF7	4.50	PSTPIP2	5.27	GBP2	6.61
CCL7	4.42	BATF2	5.24	HAPLN3	6.35
PSTPIP2	4.41	LOC100133583	5.19	ZBP1	6.28
HAPLN3	4.31	CIITA	5.13	FCGR1A	6.26
TNFSF13B	4.31	METTL7B	5.11	SOD2	6.24
FCGR1C	4.28	NFIX	5.08	MGC33556	6.08
BATF2	4.28	CD40	4.94	GIMAP7	6.00
TAP1	4.27	GIMAP4	4.92	NCF1C	5.99
IL15RA	4.21	SDS	4.91	FCGR1B	5.93
PARP14	4.21	SLAMF8	4.86	GIMAP8	5.93
HLA-DOA	4.20	STAT1	4.81	APOBEC3G	5.89
IFITM3	4.18	HLA-DQB1	4.80	PSTPIP2	5.89
LOC100133583	4.14	NCF1	4.77	STAMBPL1	5.89
TNFAIP6	4.10	IFI35	4.75	HLA-DPA1	5.87
CD38	4.07	TAP2	4.75	GK	5.82
HLA-DQA1	4.04	TNFSF13B	4.61	FPR1	5.76
SOD2	3.98	WARS	4.59	TAP1	5.71
LOC100133678	3.94	PSMB9	4.59	GIMAP6	5.49
METTL7B	3.93	CFB	4.56	LAP3	5.47
TYMP	3.91	TNFAIP6	4.45	LRRK2	5.41
GIMAP7	3.89	LOC389386	4.37	NFIX	5.36
CD274	3.87	IFITM2	4.18	MX1	5.34
CFB	3.87	FCGR1B	4.08	CCL7	5.26
ETV7	3.85	FAM107A	4.04	METTL7B	5.20
TNF	3.85	GK	4.03	OTOF	5.15
PSME2	3.81	TYMP	4.03	SCO2	5.11
GIMAP6	3.76	IL15RA	4.01	FGL2	5.11
GIMAP4	3.69	ECGF1	3.98	GVIN1	5.08
MGC33556	3.68	C21ORF7	3.98	ANKRD29	5.08
C1QC	3.65	APOBEC3A	3.91	CD69	5.06
MX1	3.64	APOL2	3.90	HLA-DPB1	5.06
IFI35	3.62	ITGB7	3.89	PARP14	5.06
LAP3	3.61	TMEM149	3.81	BATF2	5.05
GVIN1	3.59	CD274	3.81	CFB	4.97
XAF1	3.59	PSME2	3.81	LOC652616	4.97
GRIN3A	3.56	HLA-DPA1	3.79	CXCL10	4.95
TAP2	3.55	IL18BP	3.75	RSPO3	4.95
ANKRD29	3.54	C17ORF87	3.74	ADM	4.94
STX11	3.54	NCF1C	3.74	C17ORF87	4.93
LOC389386	3.51	SLAMF7	3.72	TAP2	4.93
ECGF1	3.50	XAF1	3.72	STX11	4.93
SEMA4D	3.48	NAMPT	3.69	IFI35	4.89
GIMAP5	3.46	SLC2A6	3.66	SLAMF8	4.80
OAS2	3.45	LINCR	3.64	XAF1	4.77
HLA-DPB1	3.45	CASP1	3.63	APOL2	4.73
NOD2	3.44	GRIN3A	3.63	SP140	4.69
IFI27	3.44	GIMAP5	3.63	SEMA4D	4.63
IFITM2	3.44	FAM20A	3.62	OAS2	4.60
LRRK2	3.40	PARP14	3.61	JAK2	4.60
LINCR	3.37	C1S	3.59	C1QB	4.53
ITGB7	3.37	GIMAP6	3.58	COLQ	4.53
FPR1	3.37	CD38	3.58	SAMD9L	4.49
LOC728744	3.36	CASZ1	3.54	GIMAP4	4.42
SP140	3.36	FCGR1A	3.54	LINCR	4.42

Table S4. Top 100 upregulated genes in IFN-γ treated macrophages. The fold change in mRNA levels, relative to carrier treated cells, for the top 100 IFN-γ -induced genes is given.

Donor 1		Donor 2		Donor 3	
Gene:	Fold change	Gene:	Fold change	Gene:	Fold change
TYMS	0.14	OLR1	0.19	KIAA0101	0.18
KIAA0101	0.15	COLEC12	0.19	PRC1	0.21
UBE2C	0.16	GPD1	0.20	VWF	0.25
CDC20	0.16	TPD52L1	0.21	PODXL	0.25
CDC2	0.16	EBI2	0.21	E2F2	0.25
PRC1	0.17	KIAA0101	0.23	GPD1	0.25
TNFRSF21	0.17	MXD4	0.23	UBE2C	0.25
TOP2A	0.17	FSCN1	0.23	SLC25A29	0.27
SLC16A10	0.18	GPR34	0.23	NCAPG	0.27
NCAPG	0.20	TYMS	0.23	TOP2A	0.28
DLGAP5	0.20	VWF	0.24	FSCN1	0.29
STMN1	0.21	PDE3B	0.25	CDC20	0.29
HMMR	0.21	STMN1	0.25	LOC642755	0.30
VWF	0.21	AKR1C3	0.26	C11ORF45	0.30
CDCA5	0.22	PODXL	0.26	MXD4	0.30
GPR34	0.22	XYLT1	0.26	NUDT7	0.31
CCNB2	0.22	SLC16A10	0.26	DPYSL3	0.31
SCG5	0.23	TIMP3	0.27	FBXO38	0.31
HIST1H4C	0.23	PRC1	0.27	CDC45L	0.31
TTK	0.23	CD300LB	0.28	HMMR	0.32
NUDT7	0.23	TMEM158	0.28	CDC2	0.32
NUSAP1	0.23	CXCR5	0.28	DLGAP5	0.32
CCNE2	0.23	MGC52282	0.28	TMEM151A	0.32
CDC45L	0.24	SEL1L2	0.29	SLC16A10	0.32
CEP55	0.24	TOP2A	0.29	OLR1	0.33
AKR1C3	0.24	FBXO38	0.29	DEXI	0.33
FSCN1	0.25	CDC20	0.29	PDE3B	0.33
SLC25A29	0.25	PHACTR1	0.29	TMEM158	0.34
COLEC12	0.25	RGS2	0.30	EBI2	0.34
RGS2	0.26	LOC642755	0.30	GPR34	0.34
PHACTR1	0.26	TSPAN13	0.32	NUSAP1	0.34
EBI2	0.26	CDC2	0.32	RGS2	0.34
PDE3B	0.26	FAM179A	0.32	USP2	0.35
CERK	0.26	UBE2C	0.32	GINS2	0.35
GINS2	0.27	RGS18	0.32	CXCR5	0.36
MXD4	0.27	TMEM45A	0.32	ITGB1BP3	0.36
CAMP	0.27	DPYSL3	0.32	TLR5	0.36
BUB1	0.28	KCNJ1	0.32	MYH10	0.36
CKAP2L	0.28	DCAF6	0.32	ASPM	0.37
MAD2L1	0.28	NUDT7	0.33	CERK	0.37
E2F2	0.28	CERK	0.33	SVIL	0.37
LOC642755	0.28	DLGAP5	0.33	TYMS	0.37
GPER	0.28	ITGB1BP3	0.33	SLC45A3	0.37
MCM7	0.29	ATP9A	0.33	CDKN3	0.38
DEXI	0.29	LOC100129882	0.33	HIST1H4C	0.38
PODXL	0.29	CDC45L	0.34	FAM179A	0.38
NEK2	0.29	METTL7A	0.34	ITGA3	0.38
ASPM	0.29	CCNB2	0.34	AKR1C3	0.38
TPD52L1	0.29	LPL	0.34	CEP55	0.38
CDKN3	0.30	TNFRSF21	0.34	STMN1	0.39
KIF11	0.30	E2F2	0.34	CENPM	0.39
DPYSL3	0.30	OPN3	0.34	MRGPRF	0.39
LPL	0.30	DEXI	0.34	GPER	0.39
TMEM151A	0.30	ZFP36L1	0.35	MCM10	0.39
FBXO38	0.30	SLC25A29	0.35	TPD52L1	0.39
METTL7A	0.31	BNIP3L	0.35	PHACTR1	0.39
OIP5	0.31	SLC45A3	0.35	CCNB2	0.40
CDKN2B	0.31	CXCR4	0.35	CD300LB	0.40
SDC1	0.32	NCAPG	0.35	ZFP36L1	0.40
BNIP3L	0.32	SCG5	0.36	CDCA5	0.40
TMEM97	0.32	FAM13A	0.36	TMEM97	0.40
UBE2T	0.32	CD14	0.36	XYLT1	0.40
HMGB2	0.32	MYH10	0.36	CLEC12A	0.40
MCM4	0.32	NUSAP1	0.36	KRT79	0.40
MCM10	0.33	GREM1	0.36	CKAP2L	0.41
AMDHD1	0.33	TMEM151A	0.37	SLC30A3	0.41
C11ORF45	0.33	STK39	0.37	CCNE2	0.41
TK1	0.33	PDK4	0.37	HAMP	0.42
GPD1	0.33	CAMP	0.37	SCG5	0.42
ITGA3	0.34	GPER	0.37	PHF19	0.42
ZFP36L1	0.34	CLINT1	0.37	METTL7A	0.42
CENPM	0.34	LOC646347	0.37	SNAI3	0.43
ANLN	0.34	CLIP4	0.38	ATP9A	0.43
CCNA2	0.34	SPARC	0.38	SYNGR1	0.43
ALOX5AP	0.34	HS.371609	0.38	BCL11A	0.43
FAM179A	0.34	C11ORF45	0.38	MFAP4	0.43
TMEM158	0.34	OLFML2B	0.38	C3ORF54	0.43
ITGB1BP3	0.34	CCND2	0.38	AGRP	0.43
CCNB1	0.34	ABHD7	0.38	DCAF6	0.44
CD300LB	0.34	TTC3	0.38	CAPN11	0.44
EXO1	0.35	SMS	0.38	MCM2	0.44
XYLT1	0.35	KIAA1147	0.38	ABCC5	0.44
SLC30A3	0.35	TLR5	0.38	C7ORF68	0.44
NCK2	0.35	ACOT2	0.39	PNPLA7	0.44
DCAF6	0.35	CLEC12A	0.39	COLEC12	0.44
CEP70	0.36	CEP55	0.39	TTK	0.45
C19ORF59	0.36	GADD45A	0.39	TFPI	0.45
GOLGA7B	0.36	SVIL	0.39	RAP1GAP	0.45
ATP8B4	0.36	CAPN11	0.39	CDH23	0.45
USP2	0.36	LOC653752	0.39	LOC100134134	0.45
RAP1GAP	0.36	CDCA5	0.39	STX2	0.45
ACOT2	0.36	DPYSL2	0.39	FNBP1L	0.45
TTC3	0.36	STS-1	0.39	UBE2T	0.45
SPARC	0.36	CDH23	0.39	KIF11	0.45
OLFML2B	0.36	ADD3	0.39	TDRD9	0.45
CCDC34	0.36	AMDHD1	0.40	GFOD1	0.45
LFNG	0.36	C7ORF68	0.40	UTS2	0.46
FAM13A	0.36	BRI3BP	0.40	ME3	0.46
NOTCH3	0.37	HSPA1A	0.40	EXO1	0.46
TNFSF14	0.37	AMICA1	0.40	CTDSPL	0.46

Table S5. Top 100 downregulated genes in IFN-γ treated macrophages. The fold change in mRNA levels, relative to carrier treated cells, for the top 100 IFN-γ -repressed genes is given.